Anti-inflammatory Effects and Biodistribution of Cerium Oxide Nanoparticles

Suzanne Marie Hirst

Thesis submitted to the faculty of the Virginia Polytechnic Institute and State University
in partial fulfillment of the requirements for the degree of

Master of Science

In

Biomedical and Veterinary Sciences

Christopher M. Reilly, Chair
Nammalwar Sriranganathan
M Nicole Rylander

February 4, 2010

Blacksburg, Virginia

Keywords: cerium oxide, iNOS, inflammation, oxygen defect, reactive oxygen species (ROS), free radical, nanoparticle

Anti-inflammatory Effects and Bio-distribution of Cerium Oxide Nanoparticles

Suzanne Marie Hirst

ABSTRACT

Cerium oxide nanoparticles have the unique ability to accept and donate electrons, making them powerful antioxidants. Their redox nature is due to oxygen defects in the lattice structure, which are more abundant at the nanoscale. Reactive oxygen species (ROS) are pro-oxidants whose presence is increased during periods of inflammation in the body. ROS damage tissues and cellular function by stripping electrons from proteins, lipids, and DNA. We investigated the ability of nanoceria to quench ROS *in vitro* and *in vivo,* and examined the biodistribution and biocompatibility of nanoceria in murine models. Nanoceria was internalized *in vitro* by macrophages, is non-toxic at the concentrations we investigated, and proteins, mRNA, and oxidative markers of ROS were abated with nanoceria pretreatment in immune stimulated cells as measured by western blot, real time RT PCR, and Greiss assay respectively. *In vivo*, nanoceria was deposited in the spleen and liver, with trace amounts in the lungs and kidneys as determined by ICP-MS. Using IVIS *in vivo* imaging, it appeared that nanoceria deposition occurred in lymph tissue. Histology grades show no overt pathology associated with nanoceria deposition, although white blood cell (WBC) counts were generally elevated with nanoceria treatment. Nanoceria suspect particles were seen in lysosomes from kidney samples of IV injected mice in HRTEM images. Lastly, IV nanoceria treatment appears to reduce markers of oxidative stress in mice treated with carbon tetrachloride (CCl_4) to induce ROS production. Taken together, our data suggest that nanoceria treatment has the potential to reduce oxidative stress.

ACKNOWLEDGEMENTS

I am truly thankful for all of the individuals in my life who have helped me in my pursuit of my Master of Science degree in the past two years. First and foremost I would like to thank Dr. Christopher Reilly for his assistance and tremendous generosity. Without his encouragement I would not be in the DBSP program today. He saw in me what I could not, and with his confidence in me I gained confidence in myself. I have no doubt that as a result of Dr. Reilly's help and encouragement I have grown more in the past two years than I had in all of my time as an undergraduate. Secondly, I want to thank Dr. Abigail Peairs for her unrelenting eagerness to help me progress in my graduate career. Dr. Peairs has been a spectacular model for me, never wavering in her professionalism or pursuit of scientific knowledge. Dr. Peairs, even in her lowest blood glucose state, would go above and beyond her call of duty to help me accomplish anything in the laboratory. She has been a great mentor and friend and I honestly do no think I could have gotten this far without her.

Dr. Sudipta Seal and Ajay Karakoti were the cornerstones of all of my research. They continually provided me with the materials, ideas, and assistance that contributed to my studies. They are wonderful collaborators whose excitement and enthusiasm for their research is refreshing. Along the same lines is Dr. Nammalwar Sriranganathan (Dr. Nathan), who is truly dedicated to his work and the "pursuit of truth." Dr. Nathan could almost always be found at his desk, engrossed in his work, yet willing to offer much-needed advice and a good, hearty laugh. Dr. Nathan has a passion to guide and teach students constructively, even if it means letting them make mistakes. Dr. M Nicole Rylander is yet another upbeat personality in an unmerciful scientific field. I admire her

for her intelligence and intense motivation to produce high-quality research. Despite her busy schedule, Dr. Rylander was still able to create time to help lead me in the right direction.

I have a long list of people with whom I may not have worked on a regular basis, but who helped me tremendously in my research. They include Melissa Makris in flow cytometry, Kathy Lowe and Dr. Tom Caceci in electron microscopy, Dr. Geraldine Magnin-Bissel in toxicology, Mike Brosius in the soils laboratory, Jeff Parks in environmental engineering, Ron Tyler and his cell counting skills, all of the dedicated CMMID personnel, and anybody else I might have accidentally left out.

Finally, as important as it is to receive professional guidance during one's graduate studies, it is just as important to receive emotional support due to the extreme stresses of graduate life. Fortunately, I have many people I can thank who have helped me in this fashion. First, I can thank my boyfriend Christopher Rourke for his emotional stability and confidence in me. Chris always had the time to sit and listen to me whether he had any clue what I was talking about or not. In the same manner my mother and father were there for me. They listened to all I had to say despite the fact that they "have no idea what it is that I actually do." Last but most definitely not the least were the lab 217 folk and many of my "kayaking friends." These friends added fun, vitality, and most importantly balance to my day.

I have been greatly blessed to be surrounded by such wonderful people. I am going to miss everyone when I move, and it will be impossible for me to forget how everyone that was a part of my life for the past couple of years has witnessed and contributed to my growth as an individual. Thank you.

TABLE OF CONTENTS

Chapter **Page No.**

LIST OF FIGURES

Figure **Page No.**

LIST OF ABBREVIATIONS

8-OH-dG – 8-hydroxy-2-deoxy guanosine
ANOVA – Analysis of variance
Aq - Aqueous
BSA – Bovine serum albumin
CCl_4 – carbon tetrachloride
CD14 – Cluster of differentiation
Ce - Cerium
CeO_2 – Cerium oxide
CGD – Chronic granulomatous disease
DCF – Dichlorofluorescein
eNOS – Endothelial nitric oxide synthase
ERK – Extracellular signal-regulated kinase
FITC – Fluorescein isothiocyanate
GSH – Glutathione
H&E – Hematoxylin and eosin
HRTEM – High resolution transmission electron microscopy
ICP-MS – Inductively coupled plasma mass spectrometry
IFN-γ – Interferon gamma
IL – Interleukin
iNOS – Inducible nitric oxide synthase
IP - Intraperitoneal
IV - Intravenous
JNK – Jun N-terminal Kinase
$LOO^{\bullet}$ - A peroxyl radical
LPS – Lipopolysaccharide
MAPK – Mitogen activated protein kinase
MDA - Malondialdehyde
NAC – N-acetyl cysteine
NADPH – Nicotinamide adenine dinucleotide phosphate
NF-κB – Nuclear factor kappa B
NK – Natural killer
nNOS – Neuronal nitric oxide synthase
NO – Nitric oxide
PAMP – Pathogen associated molecular pattern
PBS – Phosphate buffered saline
PD – Parkinson's disease
PI – Propidium iodide
PMA – Phorbol 12-myristate 13-acetate
PO – peroral (oral)
PS – Phosphatidyl serine
ROS – Reactive oxygen species
SAED – Selected area electron diffraction
SEM – Scanning electron microscopy
SLE – System lupus erythematosus
SLPI – Secretory leukocyte protease inhibitor
SO – Superoxide
SOD – Superoxide dismutase
TBARS – Thibarbituric acid reactive substances
TEM – Transmission electron microscopy
TGF- β – Transforming growth factor beta
TLR – Toll-like receptor
TNF-α – Tumor necrosis factor alpha
UVVis – Ultraviolet-visible spectrophotometry
WBC – White blood cell
XPS –X-ray photoemission spectroscopy
$\alpha T^{\bullet}$ - Alpha tocopherol

Chapter1

INTRODUCTION AND OVERVIEW OF RESEARCH

Inflammation is the body's complex and highly regulated response to stimuli such as physical damage, pathogens, or irritants.[1] Free radicals are often produced during inflammatory cascades, and are defined as molecules with one or more unpaired electrons in their outer orbital. Due to the presence of unpaired electrons, these molecules are highly unstable and tend to react with adjacent molecules, stripping them of electrons and consequently altering their structure and function. Free radical species produced within the cell include superoxide (O_2^-), the hydroxyl radical (•OH), nitric oxide (NO), peroxynitrite ($ONOO^-$), lipid hydroperoxides, and others.[1] In hydrophobic areas such as the plasma membrane, ROS can cause chain reactions in which the unpaired electron is passed from fatty acid to fatty acid, generating multiple free radical species, widespread damage, and ultimately cell death.[2-4] ROS and their products have been reported to play a role in the maintenance of cell homeostasis and other protective functions, but when an imbalance between ROS production and elimination occurs, cells and tissues experience oxidative stress.[5] Although the precise etiology of persistently abundant ROS levels remains unknown, ROS overproduction has been linked with numerous chronic inflammatory and autoimmune diseases including atherosclerosis, rheumatoid arthritis, diabetes, multiple sclerosis, and others.[5]

Cerium is a rare earth element in the lanthanide series of the periodic table. When synthesized on the nanoscale, cerium oxide (nanoceria) nanoparticles have been suggested to decrease ROS and other mediators of chronic inflammation. Nanoparticles

are defined as any material with at least one dimension 100 nanometers in length or less. At the nanoscale, cerium oxide has a unique electronic structure due mainly to its large surface-area-to-volume ratio that creates oxygen defects.[6, 7] It is these defects, or reactive sites on the nanoceria surface that can act as sites for free radical scavenging and are currently being investigated as therapeutic interventions in biological systems.[8-10] Due to the inherent structure of cerium oxide ($CeO2_{-x}$) nanoparticles, data suggests that nanoceria may reduce cellular structural damage by scavenging and inhibiting ROS as well as other inflammatory mediators in biological systems.[11] The small size of nanoparticles results in a small surface to volume ratio, which can confer unique properties to materials. So far, their unique properties of nanoceria have been utilized in ultraviolet absorbance,[12] oxygen sensing,[13] and automotive catalytic converters.[11] Biologically, it has recently been reported that cerium oxide can act as a catalyst that mimics the antioxidant enzyme superoxide dismutase.[14] Additionally, the ability of engineered cerium oxide nanoparticles to confer neuronal,[13] ocular,[15] and radioprotection[3] has been demonstrated. While previous studies report the scavenging action of nanoceria, clinically relevant parameters such as the biological mechanism, toxicological limits of dosage, bio-distribution and histopathology of nanoceria uptake have not been reported.

In our studies, we sought to define cellular uptake (in vivo and in vitro) mechanisms, biocompatibility, and to test the ability of nanoceria to decrease inflammatory mediator production in immune stimulated cells. We also examined bio-accumulation, organ deposition, clearance mechanism, histology, WBC counts, and markers of oxidative stress to determine target organs, immunologic response of, and *in vivo* scavenging of nanoceria.

Chapter 2

LITERATURE REVIEW

2.1. Inflammation and ROS

Inflammation results in increased vascular permeability in affected tissues resulting in redness, swelling, pain, loss of function, and increased temperatures. Increased blood flow produces a large influx of inflammatory cells to sites of inflammation.[1] Both resident and recruited inflammatory cells produce a battery of mediators including reactive oxygen species (ROS) that recruit additional inflammatory cells, kill pathogens, and further activate the inflammatory cascade.

During inflammation, an array of white blood cells called leukocytes is recruited to an infected area. Vascular endothelial cells, dendritic cells, macrophages, and interstitial fibroblasts residing in affected tissues release chemokines and other soluble mediators to recruit leukocytes from circulation.[1] Chemokines and cytokines induce the production of receptors such as P-selectin, E-selectin, and integrin on the surfaces of endothelial cells that attach to carbohydrate ligands on immune cells.[16] The weak attachment of a receptor to its ligand causes the recruitment of leukocytes that accumulate and "roll" over endothelial cell surfaces and migrate into tissues in a process called chemotaxis.[16] Recruited leukocytes then produce cytokines to enhance or maintain the inflammatory response.

Some leukocytes include granulocytes such as eosinophils, basophils, neutrophils and non-granular cells such as monocytes, natural killer (NK) cells, and T and B

lymphocytes. Granular cells are often short-lived and are associated with acute inflammation, whereas non-granular cells are longer-lived and more often involved in chronic inflammation.[16] Both granular and non-granular leukocytes stem from a myeloid progenitor cell and have distinct and irreversible functions.[17] Mast cells **(Figure 2.1)** are key initiators of inflammation that permanently reside in tissues. They release reactive chemicals and enzymes such as histamine and serine proteases during degranulation. They also produce chemokines and cytokines to begin the leukocyte recruitment and activation process.[16] Neutrophils are the most abundant leukocytes in healthy humans. They are short-lived and accumulate within hours at inflammatory sites, releasing cytotoxic granules including reactive oxygen species (ROS) that cause tissue damage, yet are essential for combating bacterial and fungal infection.[16] One of the most important functions of neutrophils is their ability to phagocytize, or ingest, and digest foreign materials with toxic granules.[18] As recruited cells continue to release chemokines, cytokines, ROS, and histamines, the inflammatory cascade is further augmented. Monocytes are the circulating precursors to the long-lived tissue-resident macrophages or dendritic cells.[16] They arrive at inflammatory sites later than neutrophils and have the similar function of phagocytosis and microbial digestion, however they are very different in that they are involved in microbial recognition and immunomodulation.[1] Macrophages have been recognized as a link between the first-acting, non-specific innate immune system and the adaptive, specific immune system.[1] The remaining granulocytes including eosinophils and basophils are less abundant and are involved in immunity against parasites and allergies. Natural killer cells, named so because they do not require activation, are involved in the rejection of tumors and virally infected cells.[19] T and B

lymphocytes are essential for life, are involved in adaptive immunity, yet are not directly involved in the innate immune response.

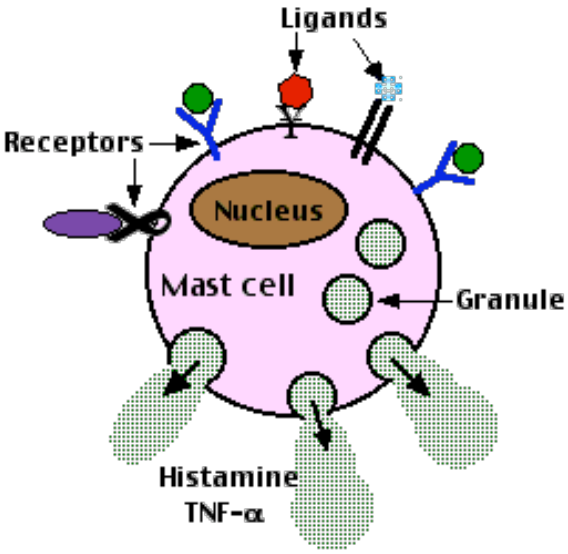

http://users.rcn.com/jkimball.ma.ultranet/BiologyPages/I/Inflammation.html

Figure 2.1 Image of a mast cell. Mast cells are key initiators of inflammation and often are the first to arrive at sites of damage or infection. Binding of specific ligands to particular cell surface receptors triggers the production of cytokines such as TNF-α and release of histamine from granule containing vacuoles.

Free radicals are often produced during inflammatory cascades of the innate immune system. They are defined as molecules with one or more unpaired electrons in their outer orbital. Many of these species are nitrogen or oxygen-containing compounds, with the oxygen species being the more detrimental and common of the two and are collectively referred to as reactive oxygen species (ROS).[2] Due to the presence of unpaired electrons, these molecules are highly unstable and tend to react with adjacent molecules, stripping them of electrons and consequently altering their structure and function. In hydrophobic areas such as the plasma membrane, ROS can cause chain reactions in which the unpaired electron is passed through multiple fatty acid carbons, generating numerous free radical species, widespread damage, and ultimately cell

death.[2, 4] Common ROS include hydrogen peroxide, superoxide (SO or O_2^-), the hydroxyl radical (OH•), nitric oxide (NO), peroxynitrite ($ONOO^-$), and others[14] **(Figure 2.2)**. They can be disabled by protective enzymes such as super oxide dismutase (SOD) **(Figure 2.2)**, catalase, glutathione peroxidase or by nonenzymatic antioxidants such as thiols, ascorbate, and α-tocopherol.[5, 20]

Free radicals can be released dually through exocytosis of activated immune cells or as byproducts of cellular metabolism in the mitochondrion (eg. leakage from the electron transport chain). It is important to note that while ROS can result in cellular and tissue damage, its presence in low amounts is vital for organisms to maintain homeostasis.[21, 22] Neutrophils and macrophages use ROS to destroy harmful bacteria by using hydrogen peroxide (H_2O_2) made by myeloperoxidase and released during respiratory burst.[22] In the thyroid gland, H_2O_2 generated by nicotinamide adenine dinucleotide phosphate (NADPH) oxidase in the thyroid assists a peroxidase enzyme in adding iodine to aromatic rings for the synthesis of the hormone thyroxine.[22] Hydrogen peroxide and other peroxides can either directly or indirectly help regulate gene expression of the pro-inflammatory transcription factor NF-κB.[22] Furthermore, the importance of ROS is demonstrated in a small population of individuals suffering from chronic granulomatous disease (CGD) caused by a defective gene for one of the subunits of ROS producing NADPH oxidase.[23] These individuals have a difficult time clearing themselves of bacterial infections, the result of which can be the development of a cluster of infected cells called a granuloma.

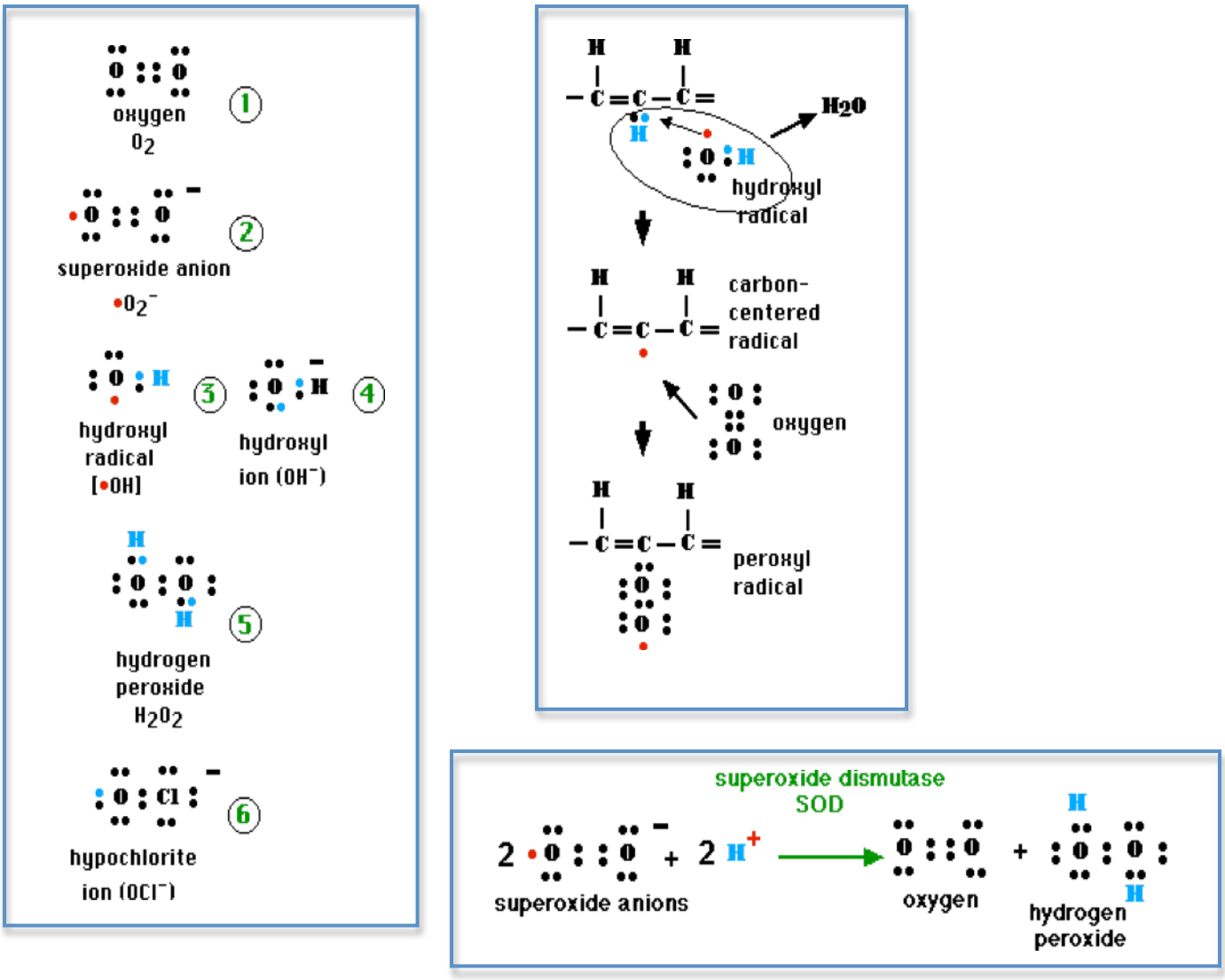

http://users.rcn.com/jkimball.ma.ultranet/BiologyPages/R/ROS.html

Figure 2.2 ROS examples and mechanisms. (left) Examples of ROS include oxygen, superoxide anions, hydroxyl radicals, hydroxyl ions, hydrogen peroxide, and the hypochlorite ion. (top right) Action of free a radical on the fatty acid side chains of a lipid. A hydrogen atom is removed by an OH radical, water is generated and the carbon atom becomes a radical. The new radical can react with oxygen to form a peroxyl radical, which can steal a hydrogen atom from a neighboring side chain thus propagating the reaction. (bottom right) The conversion of superoxide and 2 H^+ ions (more damaging) to hydrogen peroxide and water (less damaging) by the enzyme super oxide dismutase.

2.2. Oxidative stress and markers of oxidative stress

ROS and their products have been reported to play a role in the maintenance of cell homeostasis and other protective functions; however, cells experience oxidative stress when an imbalance between ROS production and elimination occurs.[5] Although the cause of oxidative stress is unknown, increased ROS levels have been linked with numerous chronic inflammatory and autoimmune diseases including atherosclerosis, rheumatoid arthritis, diabetes, multiple sclerosis, and others.[5] Abnormally high ROS levels could result from multiple mechanisms: 1) inadequate intake of food containing antioxidants or excessive intake of pro-oxidants, 2) exposure to noxious chemicals or ultraviolet light, 3) escape from mitochondrial origin during the process of oxidative phosphorylation, 4) intense exercise or particular diseases in which a hypoxic and reoxygenation process occurs inside the capillary endothelium, and 5) from uncontrolled oxidative burst from inflammatory cells.[24] Due to their labile nature and short life span, directly quantifying ROS production has been problematic, but the measurement of markers attributed to oxidative stress has been widely reported to accurately assess ROS activity.[25]

Uncontrolled oxidative burst is one of the more elusive and difficult to control mechanisms by which oxidative stress occurs. Oxidative stress has been associated with the inability of cells to efficiently regulate the activation of tissue macrophages and neutrophils and the uninhibited recruitment and activation of other phagocytic leukocytes.[26] Oxidative, or respiratory burst is a mechanism in the body's first line of defense in which phagocytes such as macrophages and neutrophils release harmful free radicals and ROS into their environment to kill foreign invaders.[27] Macrophages are the most important source of ROS because their persistent accumulation is connected with oxidative stress.[1] Oxidative burst by macrophages and neutrophils can lead to large

amounts of superoxide (SO) and hydrogen peroxide, which can result in the formation of the more highly destructive hydroxide ion through Fenton chemistry.[20] Respiratory burst is synergistic with pro-inflammatory signaling, resulting in modulation of numerous gene expression pathways. It has been shown that the NF-κB, MAPK, ERK, and JNK pro-inflammatory pathways are all activated by respiratory burst.[27]

Uncontrolled ROS can have many direct and indirect effects on cell signaling pathways that can result in cellular death via apoptosis or necrosis.[21] Probably the best characterized damage that results from ROS overproduction is lipoperoxidation. Lipoperoxidation is the oxidative modification of fatty acids (phospholipids) in cell membranes. As electrons and/or atoms are stripped from fatty acid chains, membrane fluidity, embedded protein structures, and cell signaling processes are altered.[21] Hydrogen atoms are stripped from methylene groups of fatty acids and leave behind unpaired electrons on the carbon chain. The resulting polyunsaturated fatty acids are even more prone to oxidation due to the presence of the newly formed double bond at the carbon atom. This carbon atom undergoes molecular rearrangement resulting in a conjugated diene that chain-reacts with adjacent carbon atoms until either the substrate is consumed or is terminated by a chain-breaking antioxidant.[28] Lipid peroxidation not only causes changes in membrane fluidity but also increases its permeability, membrane potential, and eventually the membrane ruptures and the cell dies.[28] One marker of oxidative stress that correlates to the amount of oxidized lipids *in vivo* is 8-isoprostane. The chain-reaction through which 8-isoprostane is generated is detailed in **Figure 2.3**.

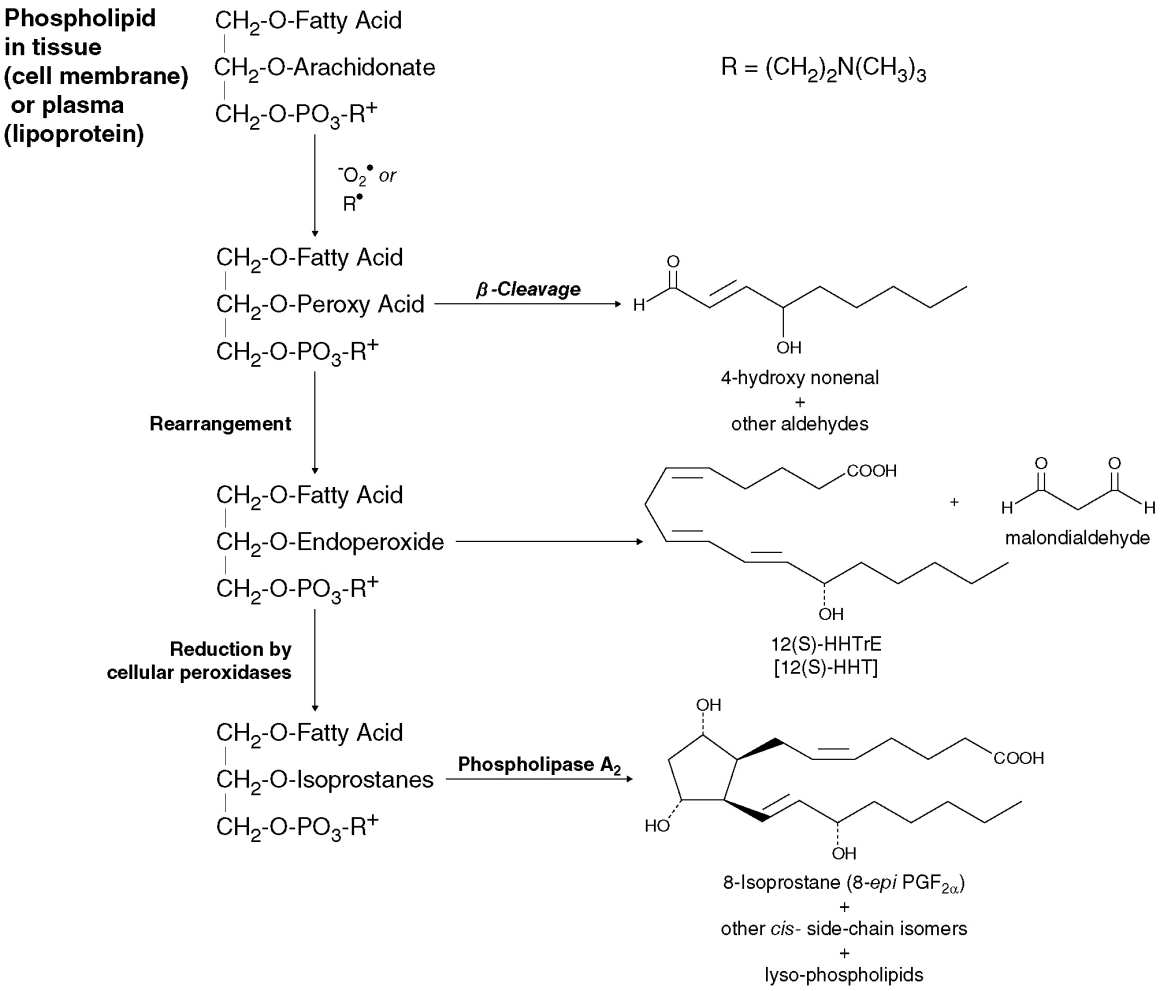

Figure 2.3 Example of lipoperoxidation and formation of 8-isoprostane.

Protein and DNA macromolecules are also targets of free radicals and ROS. Protein damage is characterized by the addition of carbonyl groups, cross-linking, or fragmentation. The oxidation of amino acids alters charges, tertiary, and quaternary structures of proteins. Changes in protein structure can result in decreased or loss of function of proteins. Just as in lipid peroxidation, oxidized proteins are increasingly subject to further oxidation and other forms of damage such as proteolysis.[28] Protein oxidation can be correlated with protein carbonyl levels. Lastly, DNA oxidation is also a common occurrence and results in conversion of DNA bases into other products, double-strand breaks, and protein/DNA cross-links. The product 8-hydroxyguanine is one of the

most reliable markers of DNA oxidative damage and is a result of the oxidation of guanine.[28] Damage to DNA can alter gene transcription leading to dysregulation of protein synthesis and inhibition of normal cellular function.

2.3. Oxidative stress and disease

Oxidative stress has been associated with various disease states.[29] The anomaly persists as to whether the role of ROS accumulation causes, is a symptom of, or is one of many contributors to disease.[29] The likelihood is that oxidative stress is a secondary phenomenon in most diseases,[22] but ROS involvement in disease is incredibly complex, and it is also very possible that all three roles are involved in any one of a number of diseases.[29] Despite the argument as to whether ROS causes or mediates disease, it remains undisputed that ROS play a major role in the progression of numerous diseases by causing damage and dysfunction of DNA, lipids, and proteins.

Diseases associated with ROS include but are not limited to neurological, autoimmune, and cardiovascular origins. There are numerous examples of diseases associated with oxidative stress including Alzheimer's disease, rheumatoid arthritis, atherosclerosis, diabetes, Parkinson's disease, systemic lupus erythematosus (SLE), ulcerative colitis, and others.[22, 29-32] Rheumatoid arthritis is a fairly common autoimmune disease (1% of the U.S. population) and is a systemic inflammatory reaction with hyperplasia of synovial tissues leading to cartilage, bone, and ligament damage.[32] ROS, NO, cytokines (mainly TNF-α), and prostaglandins are pro-inflammatory mediators that have been implicated as indicators that contribute to joint pathology in disease. Localized oxidative stress coupled with low levels of the protective enzyme superoxide dismutase (SOD) in synovial fluid has been found in arthritis patients.[32] ROS damage to

endothelial cells can increase the permeability of microvasculature, resulting in a cascade of inflammatory reactions including the migration of pro-inflammatory neutrophils and macrophages to affected areas.[32] Oxidative stress, inflammation, and mitochondrial dysfunction have also been found to contribute to dopamine cell degeneration in Parkinson's disease (PD).[31] This has been confirmed by not only postmortem studies but also studies demonstrating nigral cell degeneration via oxidative stress. Evidence supporting that levels of basal oxidative stress in substantia nigra pars compacta (SNc) are elevated in PD also exists.[31] While the etiology of oxidative stress remains unclear, it is obvious that overabundant levels of ROS disrupt cellular homeostasis, interfering with critical biochemical processes causing cellular dysfunction.

2.4. Therapeutics to modulate ROS

It is essential that all organisms be able to compensate for damage caused by ROS in order to survive in an oxygen rich atmosphere.[33] There are three main concepts of defense against ROS and free radicals. The first is prevention of the formation of or exposure to ROS.[33] Examples include avoiding ultra violet sunrays and maintaining the complex packaging of DNA in chromatin (thereby lessening exposure of genetic material to ROS).[33] The second concept is repair from ROS damage. Organisms have evolved numerous enzyme systems for DNA repair in addition to lipolytic and proteolytic enzymes capable of restitution or replenishment.[33] The last major mechanism of protection is interception between ROS and their DNA, protein, and lipid targets.[33] This last mechanism is accomplished with antioxidants that are often used as oxidative stress therapies.

ROS interception can occur with either enzymatic or non-enzymatic antioxidant molecules that are oxidized by ROS and other free radicals, resulting in less or no

damage to the organism.[22] The body can produce many of its own enzymatic antioxidants, while non-enzymatic antioxidants may be obtained through diet. It is important to note that non-enzymatic antioxidants must be continually replenished, and that a balance of lipid soluble and water-soluble antioxidants must be maintained to protect the body from oxidative damage.[24] Tocopherols (vitamin E), carotenes **(Figure 2.4)**, oxy-carotenoids, vitamin A, and ubiquinols are important lipid phase antioxidants. α-Tocopherol is the most important antioxidant within membranes and lipoproteins.[22] It functions by scavenging peroxyl radical ($LOO^{\bullet}$) intermediates and producing the less reactive α-tocopherol radical ($\alpha T^{\bullet}$) through the reaction

$$\alpha TH + LOO^{\bullet} \rightarrow \alpha T^{\bullet} + LOOH,$$

which ultimately slows the chain reaction of lipid peroxidation.[22] On the other hand, ascorbate (Vitamin C) **(Figure 2.4)**, glutathione, and other compounds are soluble in the aqueous phase. Ascorbate may react with $\alpha T^{\bullet}$ at the surface of membranes and lipoproteins and may regenerate α-tocopherol.[22] Antioxidants may completely quench a radical species, regenerate another antioxidant, or deactivate a free radical into a less harmful ROS, such as through the conversion of superoxide to hydrogen peroxide by the enzyme superoxide dismutase (SOD).[22] It is with many of these antioxidants that therapies for chronic inflammation and oxidative stress have been developed.

Some established dietary antioxidants are routinely prescribed or recommended as treatments or prevention of disease. For example, α-Tocopherol is an essential antioxidant in humans and has been shown to slow development of atherosclerosis in adults and diminish the risk and/or effects of retinopathy in premature infants.[22] It is

possible that vitamin C can regenerate vitamin E after its oxidation, and it has been thought to react preferably with pollutants such as ozone (O_3), cigarette smoke, and nitrite in the respiratory tract.[22] Flavenoids, abundant in wine, are plant phenols that have been demonstrated to inhibit lipid peroxidation and lipoxygenase enzymes (*in vitro*) and may explain the "French paradox," including why some physicians recommend a glass of wine a day.[22]

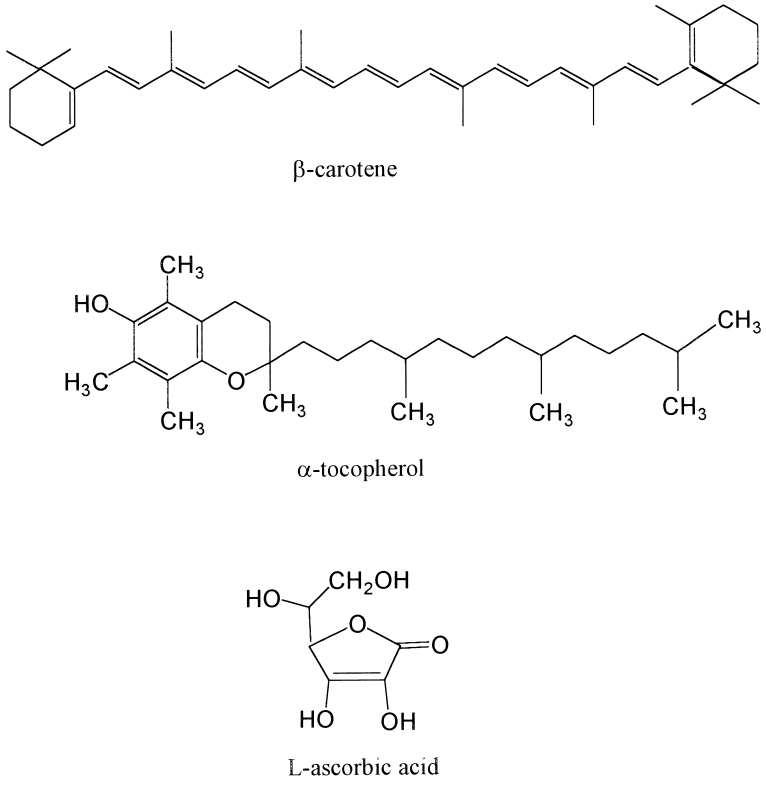

Figure 2.4 Examples of antioxidant vitamins.

N-Acetyl Cysteine (NAC) is a widely used antioxidant administered orally or intravenously, and is used most often to treat acetaminophen poisoning in humans.[34, 35] NAC is an acylated (to make it water soluble) version of the amino acid L-cysteine. In the body, L-cysteine is obtained from L-cystine, which is essentially an L-cysteine dimer

(**Figure 2.5**). Cysteine is the limiting amino acid used in the production of glutathione (GSH), which needs only three amino acids to function: glutamic acid, cysteine, and glycine.[36] GSH is the predominant anti-oxidant in the aqueous cytoplasm of cells, produced primarily in the lungs and liver.[36] In addition to its antioxidant activity, NAC has also been shown to inhibit pro-inflammatory NF-κB by intercepting multiple pathways (TNF, IL-1, LPS and PMA) and has been proposed as a supplement for the treatment of individuals with HIV.[37] NAC has been proposed as a promising therapeutic agent in reducing endothelial dysfunction, inflammation, fibrosis, invasion, cartilage erosion, and transplant prolongation due to its non-specific reducing activity and multiple methods of action.[38]

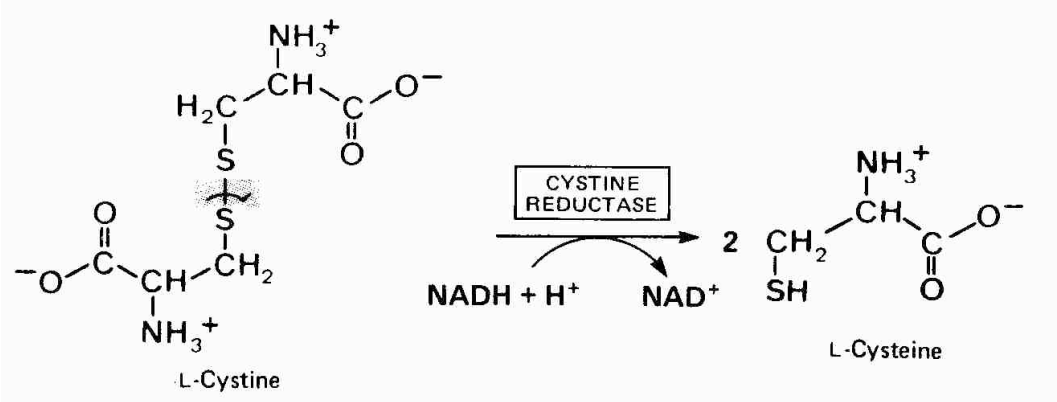

Figure 2.5 Formation of L-Cysteine from L-Cystine. L-Cystine is unstable and not very water-soluble, therefore the main extracellular source of intracellular cysteine is the dipeptide cystine. The enzyme cystine reductase catalyzes the formation of L-Cysteine needed for glutathione production by oxidizing NADH to NAD^+ and breaking up the L-Cystine dipeptide.

2.5. Cerium oxide nanoparticles

Nanoparticles are defined as any material with at least one dimension to be 100 nanometers in length or less. The small size of nanoparticles results in a large surface area to volume ratio, which can confer unique properties to materials.[9] Cerium oxide

(CeO_2) nanoparticles (nanoceria) are generated from an oxide of a rare earth metal called cerium (Ce). The term "rare earths" was applied to a group of metals originally found in the earth's crust in uncommon minerals. The metals are actually quite common, with Ce being the 25th most abundant element in the crust. On the nano scale, cerium oxide exhibits unique antioxidant properties that have thus far been found to confer radio,[3] neuro,[39] and ocular[15] protection, and have also been utilized in ultraviolet absorbance[12] and automotive catalytic converters.[11]

Nanoceria have been studied recently for their regenerative free radical scavenging abilities. Nanoceria can quench free radicals by switching between its 3+ and 4+ oxidation states, offering up electrons to ROS and other free radicals. Its regenerative properties are due to its ability to use water or other molecules to return it to a 3+ oxidation state after a scavenging event. The antioxidant properties are due, in part, to the valence structure of the cerium atom combined with inherent defects in lattice structure. Defects are areas on the surface of nanoceria particles where oxygen has been released, as nanoceria can alternate between CeO_2 and CeO_{2-x} from the uptake and release of oxygen. Surface oxygen vacancies expose the reduced and more active cerium (III) on the surface to act as reactive sites for free radicals for electron transfer from or to the nanoceria. Each nanoceria particle can have multiple defect sites and thus quench numerous radical species. The maximization of ceria in its 3+ state is necessary for optimizing its radical scavenging ability.[8] One proposed reaction involving radical quenching and regeneration is

$$Ce^{3+} + O_2^- + 2H^+ (aq) \rightarrow Ce^{4+} + H_2O_2$$

$$2Ce^{4+} + H_2O_2 \rightarrow 2Ce^{3+} + 2H^+ + O_2,$$

although other mechanisms are possible and very likely exist, such as through the use of water to regenerate itself to a 3+ state.

2.6. Role of macrophages in inflammation

Macrophages are essential initiators and mediators of inflammation and are part of the mononuclear phagocyte system.[1] There are three main functions of macrophages: antigen presentation, phagocytosis, and immunomodulation via cytokine and growth factor production.[1] Macrophages play important roles in both innate and adaptive immunity.[17]

Antigen presentation is a function of specific immune cells to help white blood cells, or lymphocytes, recognize a component of foreign material.[1] Antigens are materials capable of inducing an immune response. Antigen presenting cells can present, in context with the host's compatible antigens I and II, small pieces of an intracellular pathogen on the outer surface of their plasma membranes to lymphocytes, mainly T cells.[1] Antigen recognition by leukocytes activates the white blood cells to initiate an inflammatory cascade and destroy any pathogen or foreign material containing the exact antigen presented to them by the macrophage. This is a very specific process, meaning that each foreign "invader" has an inflammatory response specially tailored to its own antigens. This sequence of events is what is often referred to as the specificity of the adaptive immune response.[17]

Macrophages have critical functions in the innate immune response, one of which is phagocytosis. Phagocytosis involves the engulfment of solid materials by the cell membrane into an internal phagosome. Macrophages possess this function to intake foreign material such as microbial pathogens to combat disease.[1] Macrophages endocytize microbes and fuse the newly formed vesicle with lysosomes containing toxic

chemicals, ultimately killing the microbe.[1] The lysosome-endosome fused vesicle isolates the pathogen and the macrophage's own toxic chemicals from itself to avoid self destruction and host tissue damage. Phagocytosis can be triggered through the binding of cell surface receptors with ligand-coated particles from microbes.[1] Some examples of macrophage receptors include mannose, opsonin, and Toll-like receptors (TLR). Mannose receptors recognize conserved components of microbial cell walls, namely the mannose and fucose residues of glycoproteins and glycolipids.[1, 17] Opsonins include antibody-bound materials, complement proteins bound to antibody-antigen complexes, and lectin sugars bound to carbohydrates in cell membranes. TLRs bind to pathogen associated molecular pattern (PAMPs), which are cell wall components conserved across many pathogenic microbes.[40] Lipopolysaccharide (LPS) is a component of the cell wall of gram negative bacteria and is one example of a PAMP. Binding of mannose, opsonins, and PAMPs to the corresponding cellular receptors induces macrophages to phagocytize the material.[1, 17, 40] Macrophages also use phagocytosis to ingest cellular debris, helping the body recover from damage caused by an inflammatory reaction and to recycle cellular components such as amino acids and nucleotides.[1, 17]

The binding of ligands to receptors not only induces phagocytosis, but also activates macrophages to produce pro-inflammatory cell signaling molecules, microbicidal substances, and an upregulation of cell surface receptors. Macrophage activation most often occurs through the binding of cytokines and PAMPs to receptors. PAMPs such as LPS are potent macrophage activators.[17] Cytokines are soluble proteins, peptides, or glycoproteins used for cell communication during inflammatory conditions. An array of macrophage-produced cytokines promotes the killing of pathogenic microbes and the production, mobilization, activation, and regulation of numerous inflammatory

effector cells.[41] One example is interferon gamma (IFN-γ), formerly known as macrophage-activating factor, that is a cytokine produced by natural killer (NK) cells and T cells. The activation of macrophages with IFN- γ induces destruction of viruses, tumors, and cells infected with bacteria.[1] There are a number of other cytokines responsible for leukocyte and macrophage activation, many of which are produced by macrophages themselves. The cytokines interleukin 1 (IL-1), IL-6, tumor necrosis factor alpha (TNF-α), IFN-α/β, IL-10, IL-12, and IL-18 are all produced by macrophages and are involved in the regulation (up or down) of the immune response.[1, 41] IL-1 and IL-6 are both endogenous pyrogens, causing fever in the affected individual. IL-1 also results in an increase of adhesion factors on endothelial cells, increasing the number of localized leukocytes at the site of inflammation. IL-12 stimulates T cells to differentiate and produce the cytokines IFN-γ and TNF-α, in turn stimulating even more T cells and macrophages. IL-18 is part of the IL-1 superfamily and acts with IL-12 to stimulate TNF-α producing T cells and antibody producing B cells. Lastly, IL-10 is an anti-inflammatory cytokine that results in T cell deactivation, decreased antigen presentation, and deactivation of the pro-inflammatory transcription factor nuclear factor kappa B (NF-κB).

While cytokines are critical for the mediation of an inflammatory response, they do not directly kill invading pathogens. Upon ligation of PAMPs with TLRs, macrophages can undergo a process called respiratory burst. During respiratory burst, macrophages release vast amounts of reactive oxygen species (ROS).[42] ROS such as superoxide and hydrogen peroxide strip electrons from proteins, DNA, and lipids of pathogens. The removal of electrons alters a molecule's structure and function, and without the proper function of these three macromolecules, cells will either lyse or undergo programmed cell death, otherwise called apoptosis.[8]

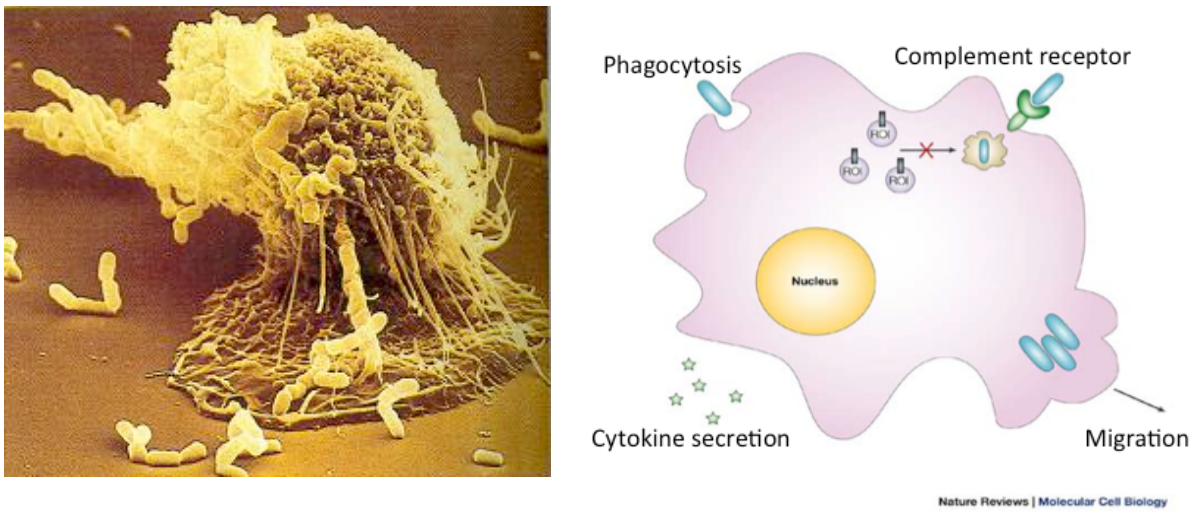

left: http://www.odec.ca/projects/2007/sank7b2/page7.html
right: http://www.nature.com/nrm/journal/v4/n5/fig_tab/nrm1104_F2.html

Figure 2.6 Images of macrophages. (left) scanning electron micrograph (SEM) of a macrophage engulfing bacteria and (right) a cartoon depiction of macrophage structures and functions.

Macrophages are not only important in the initiation and enhancement of inflammation, but they also are essential to the resolution of inflammation.[1, 43] Inflammation results in a sequence of events that can lead to tissue damage, especially if prolonged. The host must take time to recover from inflammation in order to repair damaged tissues.[43] Macrophages are responsible for the removal of debris and the deactivation of mediators and inflammatory cells. Key mechanisms involved in this process include apoptosis and the production of soluble mediators (anti-inflammatory cytokines and anti-oxidants), and direct effectors such as protease inhibitors.[1]

Apoptosis is a mechanism that induces cellular death. It is employed by inflammatory cells in order to be safely removed from sites of inflammation. Cells undergoing apoptosis are marked with certain surface receptors that trigger their engulfment by phagocytic cells.[1, 44] These surface markers are often the same receptors used in the pro-inflammatory process, including the LPS, complement, and lectin

receptors.[1] It is thought that chronic inflammatory diseases such as autoimmune disorders involve defective apoptosis or the escape of phagocytosis by pro-inflammatory cells.[1]

Soluble mediators involved in anti-inflammatory pathways include both cytokines and antioxidants. The major cytokine down regulators of inflammation produced by macrophages include IL-10 and TGF-β.[1] TGF- β initiates wound healing through the stimulation of mesenchymal cell proliferation in addition to suppressing collagenase production and increasing collagen deposition. IL-10 inhibits the production of an array of pro-inflammatory cytokines including IL-1, IL-6, IL-12, TNF-α, and others.[1, 43] It not only causes a decrease in the production of pro-inflammatory cytokines but it also increases the production of other anti-inflammatory cytokines. IL-10 also modulates chemokine and cell surface molecules by inflammatory cells.[1, 43] Antioxidants are another class of soluble mediators shown to resolve inflammation. ROS produced by macrophages act indiscriminately on targets, thereby damaging both host and pathogen structures. Enzymatic antioxidants include catalase and superoxide dismutase, catalyzing the reduction of hydrogen peroxide and superoxide, respectively.[22] Aqueous antioxidants including vitamin C and glutathione and lipid antioxidants such as vitamin E and carotenoids receive or donate electrons to ROS to form more stable or non-radical byproducts.[22] The last class of antioxidants includes the metal-binding proteins that inhibit the production of the most damaging ROS, the hydroxyl radical, by sequestering cationic iron and copper.[22] Finally, protease inhibitors are produced by macrophages to mediate tissue destruction. For example, one study found that peritoneal macrophages in mice produce secretory leukocyte protease inhibitor (SLPI) in response to the presence of apoptotic target cells.[44] SLPI is an inhibitor of numerous serine proteases and LPS

induced NF-κB and TNF-α production.[44] Consequently, macrophages play crucial roles in both pro and anti-inflammatory conditions, acting through various pathways and mechanisms.

2.7. iNOS and nitric oxide

Inducible nitric oxide synthase (iNOS) is a cytotoxic, soluble enzyme from a eukaryotic family of nitric oxide synthases (NOSs). There are at least three isoforms of NOSs including iNOS (inducible), nNOS (neuronal), and eNOS (endothelial).[45] Both n and eNOS are constitutive NOSs because they are consistently present in resting cells. Their stimulation results in the production of nitric oxide (NO), which indirectly results in the modulation of an array of mediators including various ion channels and protein kinases, and it can also modulate intracellular calcium levels. One major effect of the stimulation of constitutive NOS is the relaxation of smooth muscle.[45] iNOS, on the other hand, is not present in resting cells and is a critical host defense effector in the immune system.[45] Its production is stimulated by soluble mediators of inflammation produced by inflammatory cells or the presence of microbial products. NO production confers antimicrobial, antiparasitic, antiviral, and antineoplastic host cell activity.[46]

Activated iNOS produces the toxic free oxygen radical nitric oxide (NO) from converting L-arginine to L-citrulline using NADPH and molecular oxygen.[45] NO is a small, short-lived compound capable of diffusing freely within cells from its formation site to site of action.[45] Several mechanisms of action have been demonstrated in its alteration of biological compounds, however the main mechanism of NO involves the oxidation of iron containing proteins. NO often reacts with lipid membranes (due to concentrated oxygen), alters protein conformation by indirect reactions with thiols and amines, and can also damage DNA and carbohydrates.[45] Many different types of cells

are capable of producing iNOS, including endothelium, hepatocytes, monocytes, mast cells, macrophages, and smooth muscle cells.[45] Its production is stimulated in murine macrophages by two possible pathways: the CD14 pathway through binding of lipopolysaccharide (LPS) to CD14 receptors, and through the activation of the JAK/STAT pathway via interferon gamma (IFN-γ) binding with IFN-γ receptors.[45] On the other hand, NO production is stimulated in humans by other factors including stress, high glucose levels, estrogens, and other cytokines (TNF-α and IL-1).[46]

Low levels of NO production are beneficial in biological systems, however, overproduction of NO by iNOS is associated with inflammatory diseases such as atherosclerosis, rheumatoid arthritis, diabetes, septic shock, multiple sclerosis, etc, and its overproduction causes wide spread tissue damage.[45] NO interacts with superoxide to form peroxynitrite ($ONOO^-$) that damages proteins, lipids, carbohydrates, DNA, and carbon dioxide to produce the highly reactive nitrosoperoxocarbonate.[45] Nitrosoperoxocarbonate will change the structure and function of these macromolecules and lead to oxidative damage of tissues. $ONOO^-$ can irreversibly oxidize mitochondrial components resulting in inhibited respiration and mitochondrial dysfunction.[45] Oxidative metabolites **(Figure 2.7)** of NO can also act to inhibit antioxidants such as vitamin C, glutathione, and uric acid.[45] It is therefore thought that the prevention of the overproduction of NO can help treat disorders mediated by the free radical.

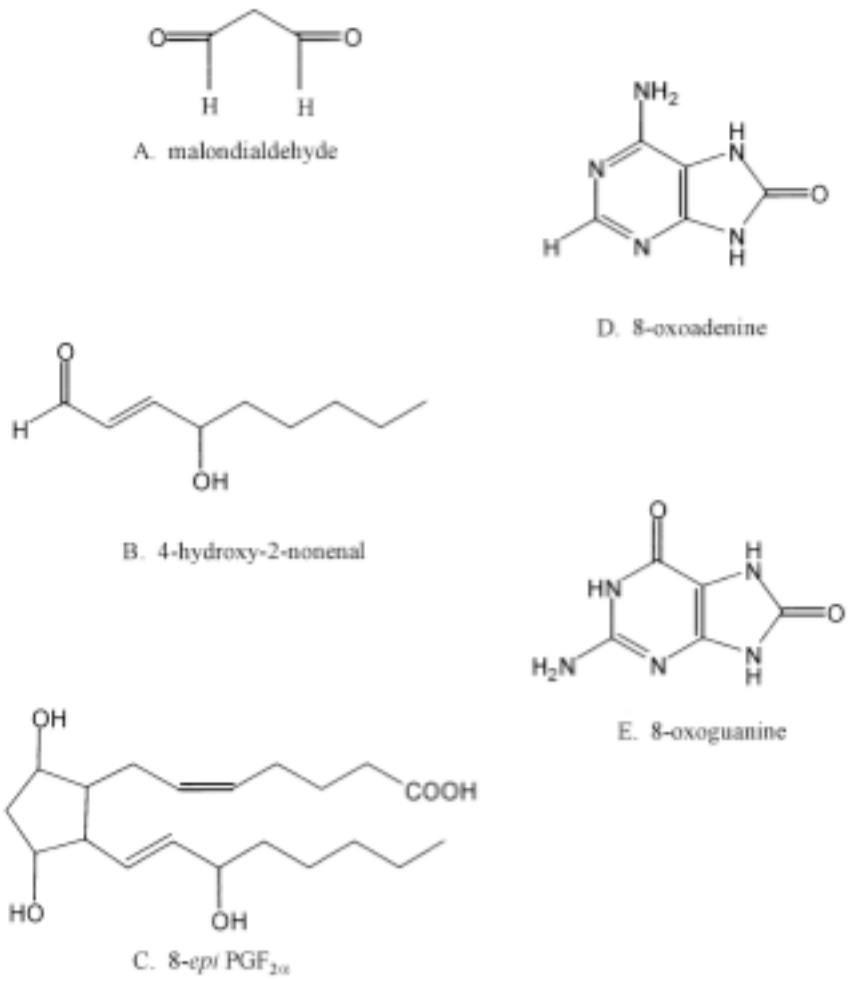

Figure 2.7 Examples of products of oxidative stress: lipid peroxidation products (A-C) and oxidized purine bases (D, E).

2.8. LITERATURE CITED

[1] N. Fujiwara, K. Kobayashi, *Curr Drug Targets Inflamm Allergy* **2005**, *4*, 281.
[2] I. P. Kaur, T. Geetha, *Mini Rev Med Chem* **2006**, *6*, 305.
[3] R. W. Tarnuzzer, J. Colon, S. Patil, S. Seal, *Nano Lett* **2005**, *5*, 2573.
[4] O. I. Shadyro, I. L. Yurkova, M. A. Kisel, *Int J Radiat Biol* **2002**, *78*, 211.
[5] I. Juranek, S. Bezek, *Gen Physiol Biophys* **2005**, *24*, 263.
[6] M. F. Hochella, Jr., S. K. Lower, P. A. Maurice, R. L. Penn, N. Sahai, D. L. Sparks, B. S. Twining, *Science* **2008**, *319*, 1631.
[7] M. Nolan, S. C. Parker, G. W. Watson, *Phys Chem Chem Phys* **2006**, *8*, 216.
[8] B. A. Rzigalinski, K. Meehan, R. M. Davis, Y. Xu, W. C. Miles, C. A. Cohen, *Nanomed* **2006**, *1*, 399.

[9] B. A. Rzigalinski, *Technol Cancer Res Treat* **2005**, *4*, 651.
[10] M. Nolan, S. C. Parker, G. W. Watson, *J Phys Chem B Condens Matter Mater Surf Interfaces Biophys* **2006**, *110*, 2256.
[11] J. C. Yu, L. Zhang, J. Lin, *J Colloid Interface Sci* **2003**, *260*, 240.
[12] S. R. Tsunekawa S, Ohsuna T, Kasuya A, Takahashi H, Tohji K., *Mater Sci Forum* **1999**, 315.
[13] M. Das, S. Patil, N. Bhargava, J. F. Kang, L. M. Riedel, S. Seal, J. J. Hickman, *Biomaterials* **2007**, *28*, 1918.
[14] C. Korsvik, S. Patil, S. Seal, W. T. Self, *Chem Commun (Camb)* **2007**, 1056.
[15] J. Chen, S. Patil, S. Seal, J. F. McGinnis, *Adv Exp Med Biol* **2008**, *613*, 53.
[16] A. D. Luster, R. Alon, U. H. von Andrian, *Nat Immunol* **2005**, *6*, 1182.
[17] S. Gordon, *Nat Rev Immunol* **2003**, *3*, 23.
[18] G. B. Ryan, G. Majno, *Am J Pathol* **1977**, *86*, 183.
[19] C. A. Biron, K. B. Nguyen, G. C. Pien, L. P. Cousens, T. P. Salazar-Mather, *Annu Rev Immunol* **1999**, *17*, 189.
[20] K. P. Pavlick, F. S. Laroux, J. Fuseler, R. E. Wolf, L. Gray, J. Hoffman, M. B. Grisham, *Free Radic Biol Med* **2002**, *33*, 311.
[21] M. A. Balboa, J. Balsinde, *Biochim Biophys Acta* **2006**, *1761*, 385.
[22] B. Halliwell, *Annu Rev Nutr* **1996**, *16*, 33.
[23] B. M. Babior, R. C. Woodman, *Semin Hematol* **1990**, *27*, 247.
[24] C. Kerksick, D. Willoughby, *J Int Soc Sports Nutr* **2005**, *2*, 38.
[25] M. B. Kadiiska, B. C. Gladen, D. D. Baird, D. Germolec, L. B. Graham, C. E. Parker, A. Nyska, J. T. Wachsman, B. N. Ames, S. Basu, N. Brot, G. A. Fitzgerald, R. A. Floyd, M. George, J. W. Heinecke, G. E. Hatch, K. Hensley, J. A. Lawson, L. J. Marnett, J. D. Morrow, D. M. Murray, J. Plastaras, L. J. Roberts, 2nd, J. Rokach, M. K. Shigenaga, R. S. Sohal, J. Sun, R. R. Tice, D. H. Van Thiel, D. Wellner, P. B. Walter, K. B. Tomer, R. P. Mason, J. C. Barrett, *Free Radic Biol Med* **2005**, *38*, 698.
[26] I. Rahman, W. MacNee, *Eur Respir J* **2000**, *16*, 534.
[27] K. E. Iles, H. J. Forman, *Immunol Res* **2002**, *26*, 95.
[28] D. J. Betteridge, *Metabolism* **2000**, *49*, 3.
[29] A. Spector, *J Ocul Pharmacol Ther* **2000**, *16*, 193.
[30] B. S. Berlett, E. R. Stadtman, *J Biol Chem* **1997**, *272*, 20313.
[31] P. Jenner, *Ann Neurol* **2003**, *53 Suppl 3*, S26.
[32] A. Mirshafiey, M. Mohsenzadegan, *Iran J Allergy Asthma Immunol* **2008**, *7*, 195.
[33] H. Sies, *Exp Physiol* **1997**, *82*, 291.
[34] G. B. Corcoran, B. K. Wong, *J Pharmacol Exp Ther* **1986**, *238*, 54.
[35] C. H. Jackson, N. C. MacDonald, J. W. Cornett, *Can Med Assoc J* **1984**, *131*, 25.
[36] G. Wu, Y. Z. Fang, S. Yang, J. R. Lupton, N. D. Turner, *J Nutr* **2004**, *134*, 489.
[37] M. Roederer, S. W. Ela, F. J. Staal, L. A. Herzenberg, *AIDS Res Hum Retroviruses* **1992**, *8*, 209.
[38] M. Zafarullah, W. Q. Li, J. Sylvester, M. Ahmad, *Cell Mol Life Sci* **2003**, *60*, 6.
[39] D. Schubert, R. Dargusch, J. Raitano, S. W. Chan, *Biochem Biophys Res Commun* **2006**, *342*, 86.
[40] C. A. Janeway, Jr., R. Medzhitov, *Annu Rev Immunol* **2002**, *20*, 197.
[41] J. Bondeson, *Gen Pharmacol* **1997**, *29*, 127.
[42] H. J. Forman, M. Torres, *Am J Respir Crit Care Med* **2002**, *166*, S4.
[43] C. N. Serhan, J. Savill, *Nat Immunol* **2005**, *6*, 1191.

[44] C. Odaka, T. Mizuochi, J. Yang, A. Ding, *J Immunol* **2003**, *171*, 1507.
[45] F. Aktan, *Life Sci* **2004**, *75*, 639.
[46] V. K. Singh, S. Mehrotra, P. Narayan, C. M. Pandey, S. S. Agarwal, *Immunol Res* **2000**, *22*, 1.

Chapter 3

Anti-inflammatory Properties of Cerium Oxide Nanoparticles

This is the pre-peer reviewed version of the following article:

Suzanne M Hirst, Ajay S. Karakoti, Ron D. Tyler, Nammalwar Sriranganathan, Sudipta Seal, and Christopher M. Reilly: Anti-inflammatory effects of cerium oxide nanoparticles. Small. 2009. Volume 5, Pages 2848-2857.

ABSTRACT

The valence and oxygen defect properties of cerium oxide nanoparticles (nanoceria) suggest that they may act as auto-regenerative free radical scavengers. Overproduction of the free radical nitric oxide (NO) by the enzyme inducible nitric oxide synthase (iNOS) has been implicated as a critical mediator of inflammation. NO is correlated with disease activity and contributes to tissue destruction. The ability of nanoceria to scavenge free radicals, or reactive oxygen species (ROS), and inhibit inflammatory mediator production in J774A.1 murine macrophages is investigated. Cells internalize nanoceria, the treatment is nontoxic, and oxidative stress and pro-inflammatory iNOS protein expression are abated with stimulation. In vivo studies show nanoceria deposition in mouse tissues with no pathogenicity. Taken together, it is suggested that cerium oxide nanoparticles are well tolerated in mice and are incorporated into cellular tissues. Furthermore, nanoceria may have the potential to reduce ROS production in states of inflammation and therefore serve as a novel therapy for chronic inflammation.

3.1 INTRODUCTION

Abnormally high levels of nitric oxide (NO) contribute to chronic inflammation, a complex immunological disorder that can result in irreversible organ damage.[1-3] Persistent inflammation frequently involves the recruitment of macrophages and lymphocytes to tissues, which often results in collateral tissue damage and necrosis with replacement by fibrosis.[4, 5] Chronic inflammation often precedes and promotes the development of many major diseases including rheumatoid arthritis, multiple sclerosis, atherosclerosis, and heart disease.[1]

Cerium oxide nanoparticles (nanoceria) have properties that can be used in nanotherapeutics to decrease mediators of chronic inflammation. So far, their unique properties have been utilized in ultraviolet absorbance,[6] oxygen sensing,[7] and automotive catalytic converters.[8] Biologically, it has recently been reported that cerium oxide can act as a catalyst that mimics the antioxidant enzyme superoxide dismutase.[9] Additionally, the ability of engineered cerium oxide nanoparticles to confer neuronal,[7] ocular,[10, 11] and radioprotection[12] has been demonstrated, while the protective mechanism has not been thoroughly investigated. This versatile biomaterial has a unique electronic structure due mainly to its large surface-area-to-volume ratio that creates oxygen defects.[13, 14] It is these defects, or reactive sites on the nanoceria surface that can act as sites for free radical scavenging and are currently being investigated as therapeutic interventions in biological systems.[15-17] While previous studies report the scavenging action of nanoceria, clinically relevant parameters such as the biological mechanism, toxicological limits of dosage, and histopathology of nanoceria uptake have not been reported.

Free radical scavenging with nanoparticles functions by inhibiting reactive oxygen species (ROS).[16-18] Free radicals are molecules that contain an unpaired electron in their outermost shell. ROS are unstable and highly reactive compounds that can strip electrons from cellular macromolecules and render them dysfunctional.[16] Chain reactions of self-propagating free radicals mediate lipid peroxidation and cause cell membrane structure damage, thereby inducing cell death.[19, 20] Free radicals are generated in low levels during normal metabolism, but production increases during diseased states, increased metabolism, and cell turnover. Free radical species produced within the cell include superoxide ($O2^-$), the hydroxyl radical (OH), NO, peroxynitrite ($ONOO^-$), lipid hydroperoxides, and others.[16] Due to the inherent structure of cerium oxide ($CeO2_{-x}$) nanoparticles, data suggests that nanoceria may reduce cellular structural damage by scavenging and inhibiting ROS as well as other inflammatory mediators in biological systems.[8] We sought to conduct an in depth study of nanoceria to define cellular uptake (in vivo and in vitro), toxicity, and test the ability of nanoceria to decrease inflammatory mediator production in immune stimulated cells.

3.2 RESULTS

3.2.1 Characterization of Cerium Oxide Nanoparticles

The characteristics of nanoparticles in terms of size, shape, and other relevant chemistry are crucial for determining the functional role of nanomaterials in biology. Therefore, in the present study, engineered nanoceria was examined using high-resolution transmission electron microscopy (HRTEM) to determine individual particle and agglomerate size **(Figure 1a).** While it is observed that the agglomerate size may range from 10 nM to 50 nM (not shown here) the individual particle size remained between 3-5

nM. The biological activity of nanoceria is proportional to the presence of mixed oxidation states, and thus the particles in solution were further examined using UVVis spectroscopy **(Figure 1b)** and X-ray photoelectron spectroscopy (XPS) **(Figure 1c)** to determine the different oxidation states. As evident from Figure 1b, both cerium (III) (transmission edge below 320 nM) and cerium (IV) (transmission edge below 430 nM) oxidation states were present in nanoceria, thereby showing that the material was well suited for further application in radical quenching. A further confirmation was obtained using XPS, which shows a relatively higher abundance of cerium in its 3+ oxidation state corresponding to the binding energy peaks at 880.2, 899.5, and 903.5 eV as opposed to those at 882.1, 888.1, 898.0, 900.9, 906.4, and 916.40 eV, which are indicative of the presence of 4+ state.

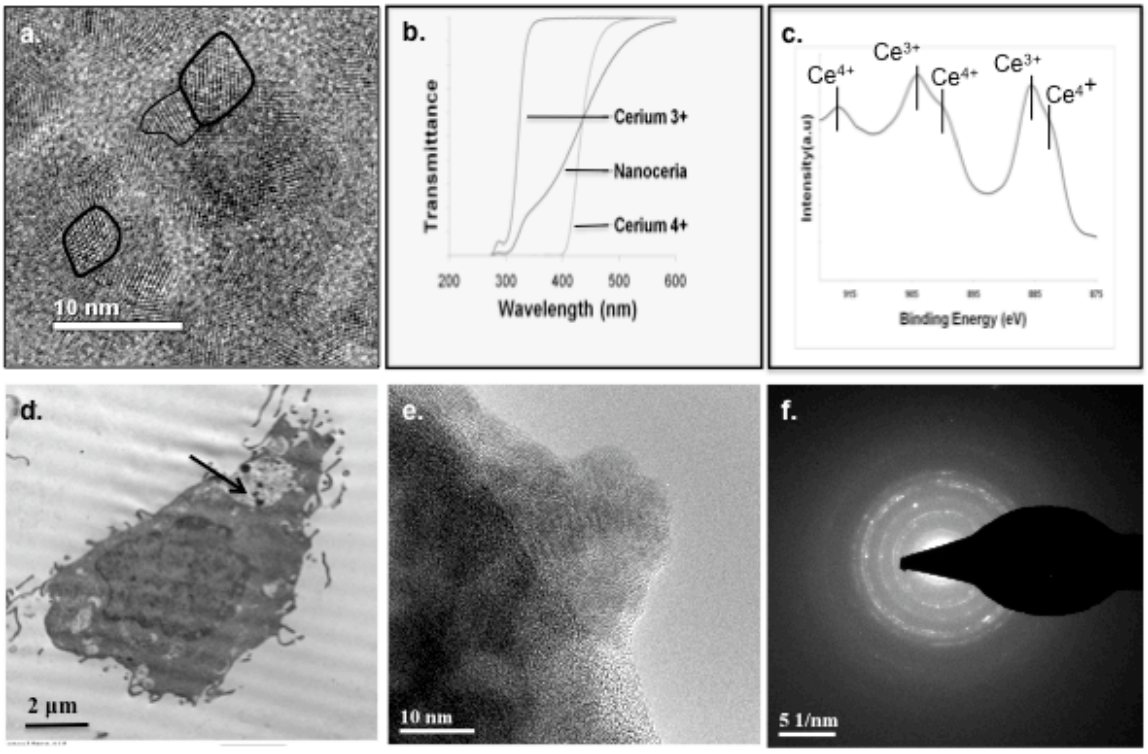

Figure 3.1. UVVis graph, XPS spectrum, and HRTEM of J774 A.1 macrophages. a) Image of ceria nanoparticles synthesized in DI water. Individual 3-5-nm particles can be

observed in 10-12-nm agglomerates confirming the presence of nanocrystallites in agglomerates. b) UVVis graph of ceria nanoparticles after one week of synthesis showing absorbance onset beyond 400 nm and complete absorbance at 300nm (cerium (III) and cerium (IV) transmission plots are shown for reference) showing the presence of both 3+ and 4+ oxidation states of ceria. c) High-resolution XPS spectrum of nanoceria showing the binding energy region of cerium, bolstering evidence of the existence of both cerium (III) and cerium (IV) species. The peaks between 875 and 895 eV belong to Ce 3d5/2 while peaks between 895 and 910 eV correspond to the Ce 3d3/2 degenerate levels. The peak at 916.4 eV is a characteristic satellite peak corresponding to cerium 4+ oxidation states. The peaks at 880.2, 899.5, and 903.5 eV are indicative of 3+ peaks as opposed to those at 882.1, 888.1, 898.0, 900.9, 906.4, and916.40 eV indicating the presence of 4+ state. d) 24 h, 10 μM nanoceria treated J774A.1 macrophages. Nanoparticles and agglomerations are present as dark, round spots between 5 and 50 nm in size. e) 24 h, 10 μM nanoceria treated J774A.1 macrophages. Clear-particle-like character could be seen in some cases. Particles are unusually small even when they are clustered. f) Selected area electron diffraction (SAED) shows the fluorite nature of the particles, confirming nanoceria uptake in macrophages.

3.2.2. Internalization of Ceria Nanoparticles

J774A.1 murine macrophage cells were used to determine if nanoceria could be incorporated intracellularly. Cells were treated with a 10 μM concentration of nanoceria for 24 h and thereafter prepared for visualization using HRTEM. Our results showed nanoceria particles and agglomerates as solid black spots localized in the phagosomes and cytosol of macrophages **(Figure 1d).** This suggests that one mechanism of uptake is through phagocytosis and that the particles may diffuse into the cytosol thereafter as we have previously shown.[21] Clusters of nanoceria between 5 and 50 nM in size were also visible on the outermost edges of the macrophages **(Figure 1e),** which leads us to believe that nanoceria may also diffuse directly through the membrane. To confirm the presence of nanoceria in the cells, we performed selected area electron diffraction (SAED), which showed the fluorite nature of the particles in cells **(Figure 1f).**

3.2.3. Biocompatibility and Limits of Nanoceria

Before measuring the ROS quenching capabilities of nanoceria in macrophages, it was imperative to investigate any cytotoxic effects that nanoceria may have. We measured programmed cell death (apoptosis) and necrosis levels of our macrophages using flow cytometry. Ten thousand cells for each sample were analyzed, cell morphology was observed, and cells were gated according to fluorescence. Early and late apoptotic cells are represented in the lower right and upper right quadrants, necrotic cells in the upper left quadrant, and healthy cells in the lower left quadrant. Morphology of ceria-treated cells was similar to controls under both non-stimulated and stimulated conditions **(Figure 2a,** only highest concentration and control shown). Likewise, there was no significant difference between apoptosis levels of control and nanoceria treated cells for either non-stimulated **(Figure 2b**) or stimulated **(Figure 2c)** cells. Our results show that nanoceria treatment elicits no toxic effects to cells at any concentration tested in this study.

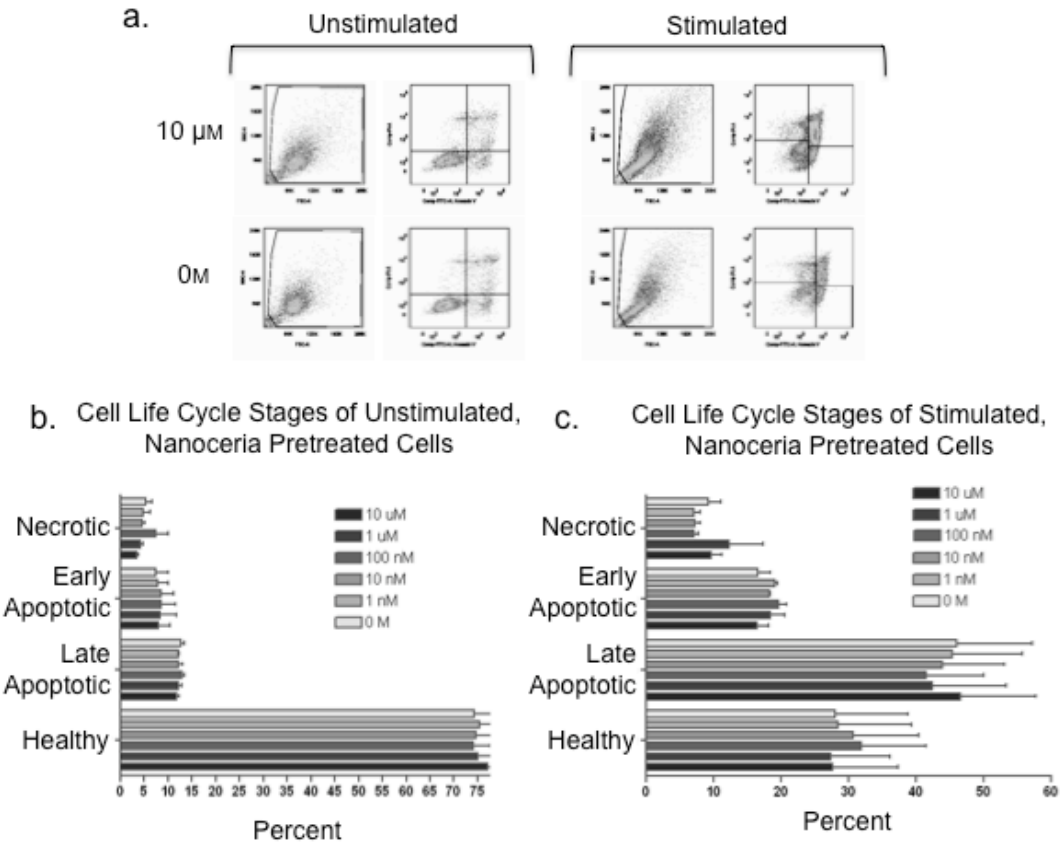

Figure 3.2. Flow cytometry to measure cytotoxicity of nanoceria. J774A.1 macrophages were assessed for apoptosis and necrosis levels using Annexin V and PI staining using flow cytometry. a) Cell morphology for nanoceria-treated, non-stimulated cells show a healthy nature (highest and lowest concentrations shown). Morphology for treated, stimulated cells is similar to that of untreated, stimulated cells. b,c) Apoptosis levels were observed and cells were gated according to fluorescence. Healthy cells are seen in the lower left quadrant, while early and late apoptotic cells are in the lower and upper right quadrants, with necrotic cells in the upper left quadrant. No significant differences in apoptosis or necrosis levels were observed in either non-stimulated or stimulated cells at any concentration. Results were analyzed using two-way ANOVA and are expressed as mean ± SEM. Significance was set at $p < 0.05$, $n = 3$. In this case $p = 1.0$ as the differences in apoptotic levels were not significantly different.

3.2.4. Conferring Protection to J774A.1 Cells Against ROS Damage

After determining that specific amounts of nanoceria could be incorporated into J774A.1 cells without inducing damage, we investigated ROS scavenging effects due to the purported antioxidant properties of cerium oxide. Initially, superoxide free radical levels

were determined by measuring chemiluminescence levels of cells using a Diogenes assay[22] specific to the detection of superoxide. Cells were pretreated for 24 h with nanoceria and subsequently stimulated in new media for another 24 h. Another set of cells were exposed to nanoceria for 24 h and then incubated in fresh medium without stimulation for 24 h. We found that chemiluminescence (directly proportional to superoxide levels) decreased almost twice the amount in stimulated cells as the concentration of nanoceria pretreatment was increased from 0 to 10 μM **(Figure 3a).** Likewise, chemiluminescence decreased as nanoceria concentrations increased in non-stimulated cells **(Figure 3b).** However, there did not appear to be an effect on the rate of radical scavenging in either the stimulated or non-stimulated states. The combined data provides direct evidence of superoxide quenching by nanoceria. Next, ROS levels were confirmed by measuring dichlorofluorescein (DCF) fluorescence using confocal microscopy. We observed a decrease in fluorescence (directly proportional to ROS levels) between 10 μM pretreated and untreated cells both with and without stimulation **(Figure 3c).** Our results from both methods of measuring ROS levels confirm the ability of nanoceria to scavenge free radicals in vitro.

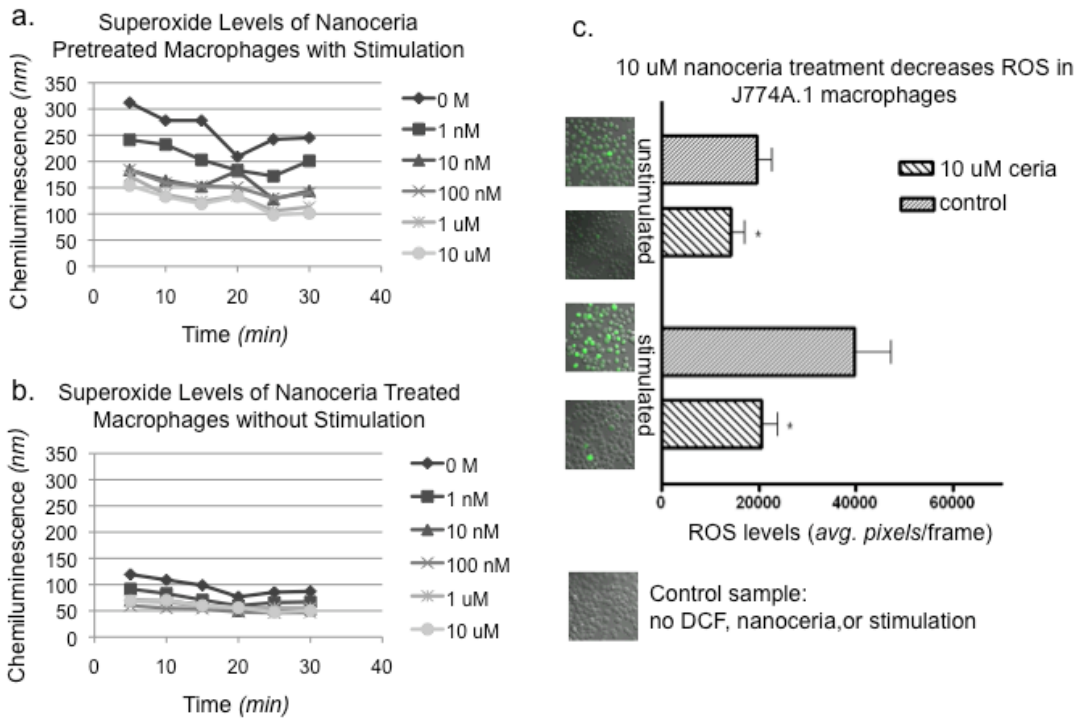

Figure 3.3. Chemiluminescence and DCF fluorescence to determine ROS levels. Cells were combined with Diogenes assay solution to measure luminescence directly proportional to superoxide production. a) Stimulated J774A.1 macrophages without a nanoceria pretreatment exhibited about twice the levels of luminescence as compared to nanoceria-treated cells of varying concentrations. b) Nanoceria-treated cells without stimulation also exhibited a decrease in superoxide production as the concentration of nanoceria treatment increased. Results are representative of four independent trials. ROS levels directly proportionate to DCF fluorescence levels were viewed. c) 24 h, 10 µM nanoceria pretreated, LPS/IFN- stimulated J774A.1 macrophages showed less DCF fluorescence than stimulated cells without a nanoceria pretreatment. 10 µM pretreated, non-stimulated cells also showed less DCF fluorescence than cells with neither stimulation nor pretreatment. Control cells exhibited no DCF fluorescence. Five random images of each sample were visualized on a Zeiss LSM510 Confocal microscope (excitation 488 nm, emission 515-555 nm) under identical parameters for each sample. Results are expressed as mean ± SEM. Significance was set at $p < 0.05$, $n = 3$. *P = 0.0293.

3.2.5. Nanoceria Suppresses iNOS Protein Levels in Stimulated Macrophages

After determining that nanoceria pretreatment decreased ROS production in J774A.1 cells, we sought to measure the protein expression of enzyme-inducible nitric oxide synthase (iNOS). Inducible NOS gene expression is upregulated in immune cells several hours after stimulation.[1] When expressed, iNOS converts arginine into citrulline and the free radical NO.[23] Increasing nanoceria pretreatment resulted in reduced expression of iNOS protein production in stimulated cells as determined by Western Blot **(Figure 4a)** and in iNOS mRNA levels in both non-stimulated **(Figure 4b)** and stimulated **(Figure 4c)** cells as determined by real-time reverse-transcriptase polymerase chain reaction (RT-PCR).

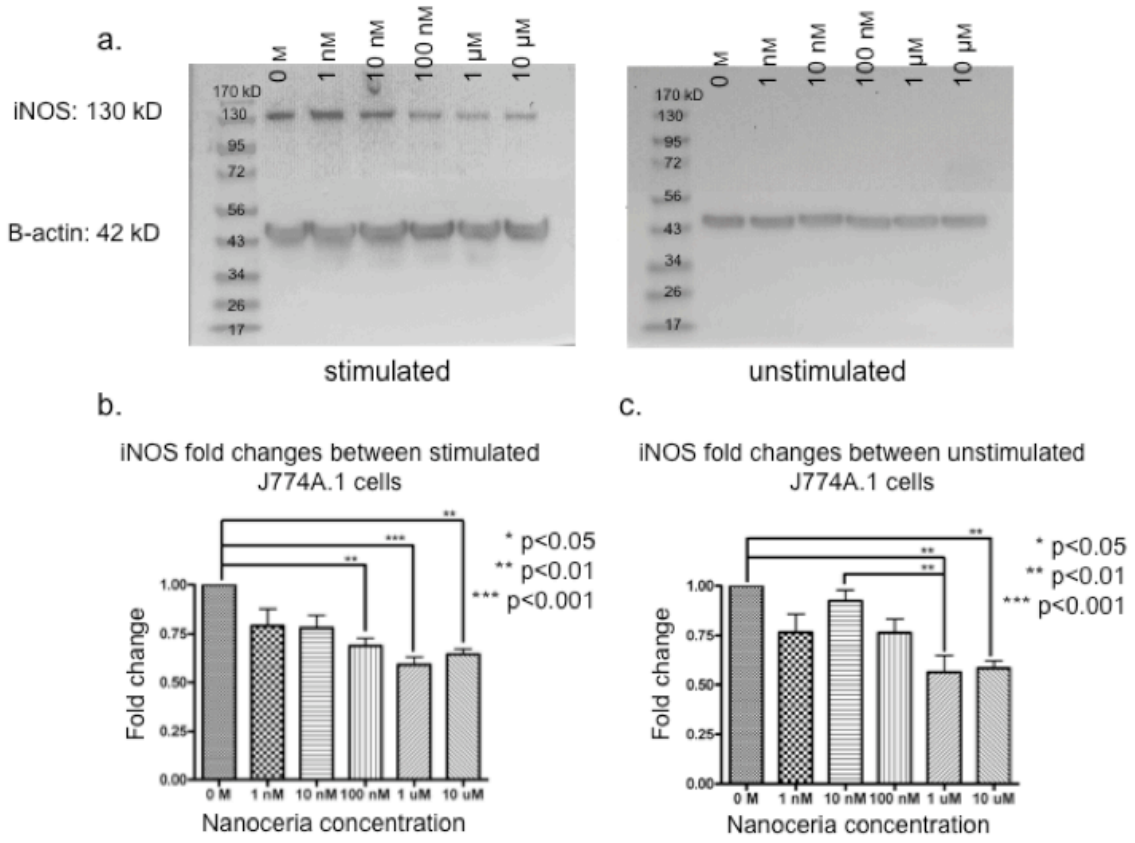

Figure 3.4. Western blot and real-time RT-PCR to measure pro-inflammatory protein production. a) Inducible NOS protein levels were measured in 24 h nanoceria-pretreated, stimulated or non-stimulated J774A.1 macrophages. Pretreatment inhibited iNOS protein production in a concentration dependent manner in cells with a subsequent 24 h

LPS/IFN- stimulation. Inducible NOS levels were unapparent in cells with subsequent 24 h incubation in non-stimulated media due to low sensitivity of the assay. Experiments shown are representative of three independent determinations. b,c) Real-time RT-PCR exhibited a decrease in iNOS levels for both stimulated and non-stimulated macrophages. Results were analyzed using a one-way ANOVA and are expressed as mean ± SEM. Significance was set at $p < 0.05$, $n = 4$.

3.2.6. Pharmacokinetics-Distribution of Injected Nanoceria Within the Body

Next, we sought to determine if nanoceria would be tolerated in vivo. We intravenously tail-injected mice with nanoceria and control mice with sterile phosphate buffered saline (PBS) solution. On day 1, group 1 (8 mice) received a low dose (0.1 mg kg-1) of nanoceria, group 2 received a high dose (0.5 mg kg-1), and the remaining control mice received PBS. Seven days post injection, 4 control mice, 4 low-dose mice, and 4 high-dose mice were necropsied and examined. The remaining mice received a repeat injection the same as day 1 on day 15. Remaining mice were then necropsied and organs harvested on day 30. Upon tissue examination by TEM, we identified small (100-200 nM), irregular electron-dense cerium oxide suspect granules dispersed within plasmoid material within tail blood vessels of the long-term high-dose mice **(Figure 5a,b)** randomly scattered within hepatocytes of the liver **(Figure 5c and d),** and in renal tubular epithelial cells **(Figure 5e and f).** High-magnification HRTEM and SAED further identified nanoceria particles in mouse tissues. Cerium oxide particle-like character can be seen in **Figure 5g,** and diffraction patterns characteristic of nanoceria further demonstrated internalization **(Figure 5h).** Histological examination of hematoxylin and eosin (H&E) stained thin sections of major organs (brain, lungs, liver, kidneys, spleen, and pancreas) showed no significant differences between 7-day-control and high-dose mice **(Figure 6a)** or 30-day-control and high-dose mice **(Figure 6b).** Specifically, no lesions were noted in the lungs, which have the largest vascular bed of any organ in the body. This is noteworthy as the

lungs have long been an area of concern in the treatment of animals with nanoparticles as deposition has been reported to lead to pulmonary embolism.[24] Therefore, nanoceria administered intravenously at both low and high concentrations was tolerated in mouse tissues and lacked evidence of overt pathogenic side effects.

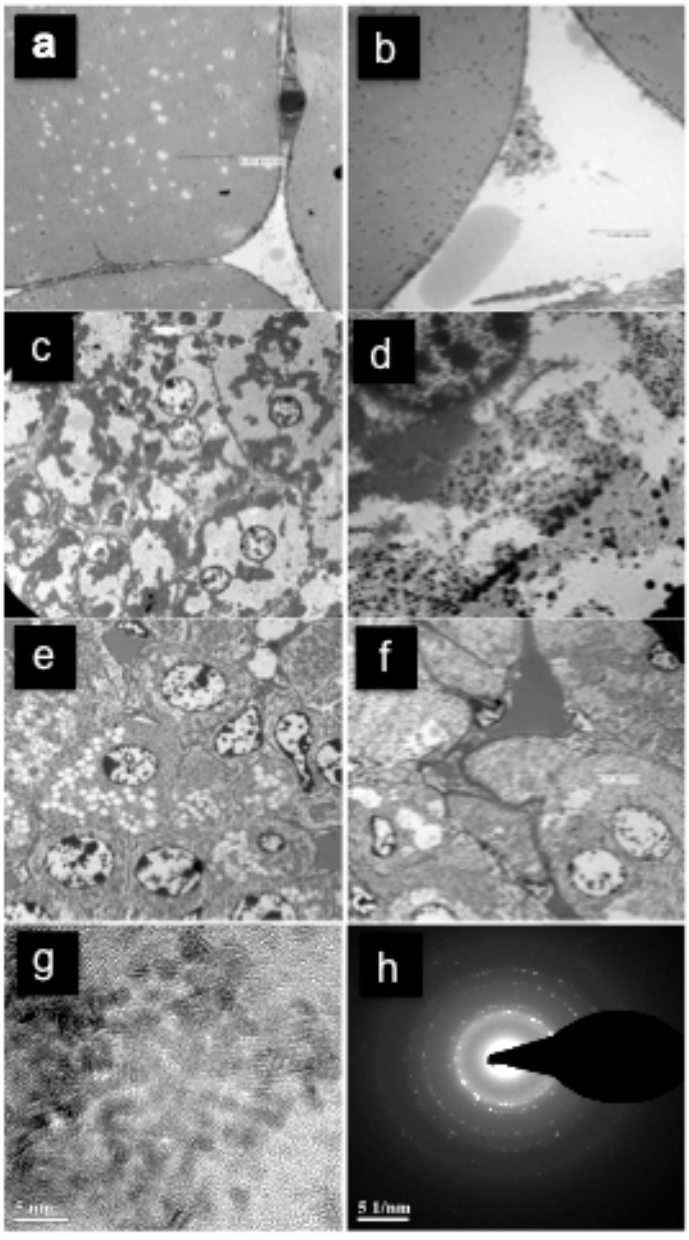

Figure 3.5. HRTEM to view nanoceria deposition in mouse tissues. Mice were exposed to 0.5 mg kg-1 dose of nanoceria via an intravenous tail injection on days 1 and 15 of an experiment. Animals were sacrificed on day 30, and tissue sections were examined using

HRTEM. a,b) Tail sections were examined and small (100-200 nm) irregular electron dense cerium oxide suspect granules dispersed within plasmoid material within tail blood vessels. c,d) Liver sections were examined; granules were found randomly scattered within the cytoplasm of hepatocytes. e,f) Kidney sections were also examined and nanoceria deposition was observed as aggregations within cytoplasm of renal tubular epithelial cells. g) High-magnification HRTEM was performed to view the nanoceria particle-like character in mouse tissues, and h) SAED demonstrated the diffraction pattern characteristic of nanoceria crystals, further evincing nanoceria deposition within mouse tissues. Images shown are representative of four independent trials.

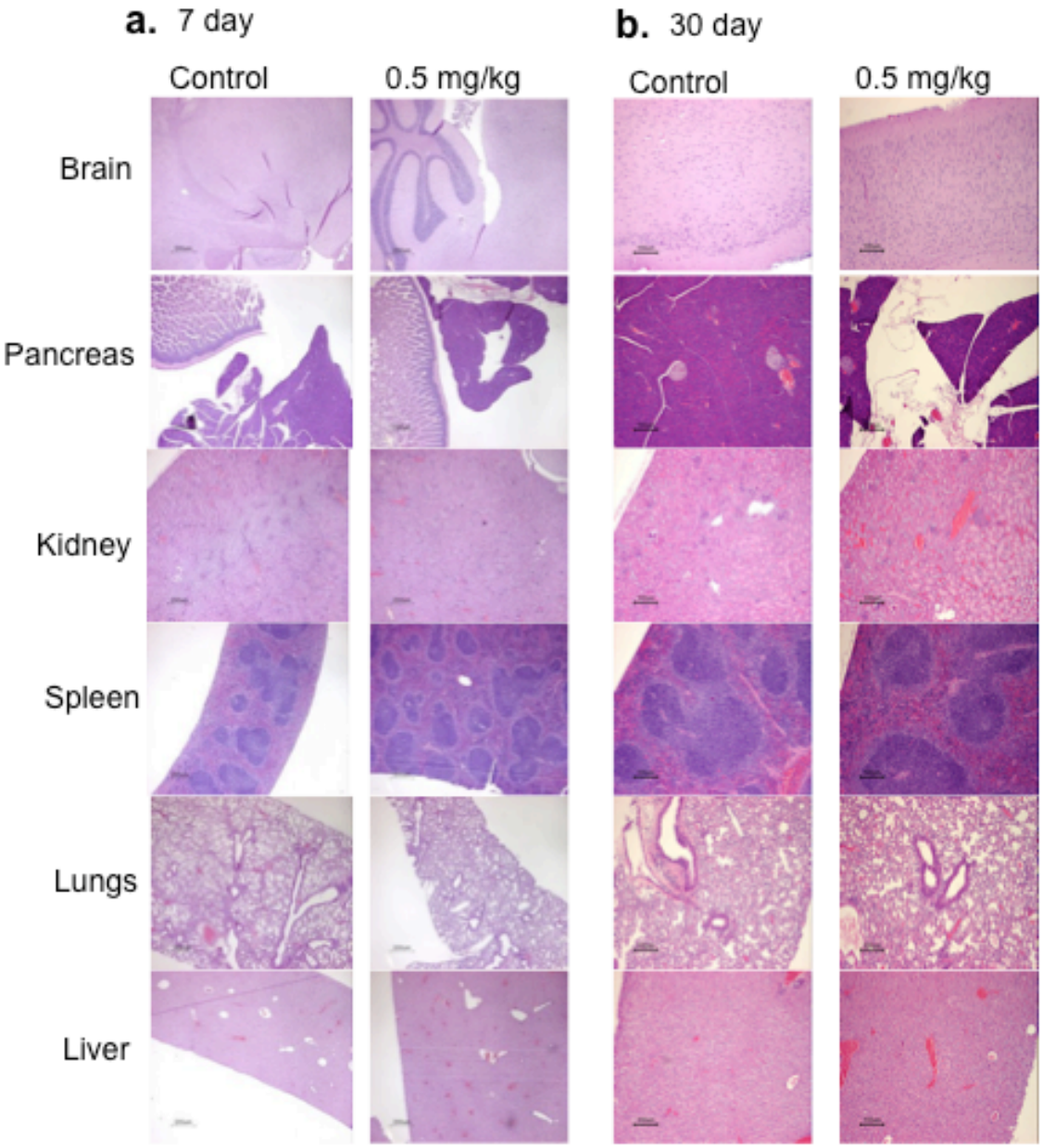

Figure 3.6. H&E staining to view side effects of nanoceria deposition. Eight mice were exposed to a 0.5 mg kg-1 dose of nanoceria via intravenous injection in the tail, and four were injected again 15 days later. The four mice receiving single injections were necropsied on day 7, and the remaining on day 30. H&E histological examination of major organs (brain, lungs, liver, kidneys, spleen, and pancreas) showed no significant difference between control and nanoceria injected mice at a) 7 and b) 30 days after injection. Importantly, no lesions were noted in the lungs, which have the largest vascular bed of any organ in the body. Images shown are representative of four independent trials.

3.3 DISCUSSION AND CONCLUSION

ROS are a major constituent of inflammation that can affect normal cellular function and have pathogenic consequences. ROS can directly damage cell membranes by oxidatively modifying fatty acid components of the phospholipid bilayer. They can also damage DNA and proteins, compromise cellular repair mechanisms, cause premature aging, and trigger apoptotic processes.[25-27] Quenching ROS production can decrease inflammation and subsequent tissue damage. In our current studies, we observed the quenching of ROS and the iNOS inflammatory mediator in immune cells by the unique scavenging ability of nanoceria. In vivo, we observed the uptake and persistence of nanoceria in mouse tissues following intravenous administration with no evidence of overt pathology (Figures 5 and 6).

The paramount characteristic of cerium oxide is its ability to scavenge free radicals, which is accomplished through its ability to reversibly switch between the 3+ and 4+ oxidation states. The reversibility of the oxidation states at relatively lower oxidation potentials also renders regenerative properties to nanoceria. These regenerative antioxidant properties are due, in part, to the valence structure of the cerium atom combined with inherent defects in the crystal lattice and oxygen defect structure.[14, 17] Ceria nanoparticles undergo easy, fast, reversible reduction to substoichiometric phases and can readily take up and release oxygen, alternating between CeO_2 and $CeO2_{-x}$.[7, 28]

Analysis of cerium oxide nanoparticles in previous studies[29] has shown that maximizing the 3+ oxidation state in nanoceria is imperative to its radical scavenging ability. In our studies, nanoceria was engineered to have both 3+ and 4+ oxidation states, which were confirmed using UVVis and XPS analysis (Figure 1b and c). A smaller individual particle size of nanoparticles ensures a higher concentration of defects and oxygen vacancy in the lattice, which can stabilize the 3+ oxidation state. Thus cerium oxide, due to its large number of defects and ability to couple in a redox manner, can quench free radicals with relative ease. Given the surface chemistry of nanoceria, there also appears to be evidence for regenerative action in situ.[7, 17, 29] The possible reactions involving the radical quenching and regeneration of oxidation states are

(1) $Ce^{3+} + \bullet O_2^- + 2H^+(aq) \rightarrow Ce^{4+} + H_2O_2$

(2) $2Ce^{4+} + H_2O_2 \rightarrow 2Ce^{3+} + 2H^+ + \bullet O_2$

Surface oxygen vacancies expose the reduced and more active cerium(III) surrounded by a pool of cerium(IV) on the surface of nanoceria particle[29] and act as reactive sites for the free radicals where electron transfer from or to the ceria nanoparticles can occur. It can also be hypothesized that immobile oxygen vacancies on the surface provide binding sites for the superoxide and peroxide species to facilitate the electron transfer processes. Redox coupling can regenerate these reactive sites so that a single ceria nanoparticle has multiple defect sites and is sufficient to quench multiple radical species. All aqueous reactions at the surface are governed by surface potential and total redox potential and thus there are many more possibilities for ceria to scavenge nearby reactive species. It must be noted that the above equations do not represent the

only mechanisms by which cerium in ceria nanoparticles may react with superoxide and hydroxyl radicals. Recent investigations also suggest that cerium ions can react with peroxide type radicals to form an intermediate peroxo-complex.[30-32] While there is no direct evidence of the formation of this peroxo-complex upon reaction of peroxide with ceria nanoparticles, spectroscopic evidence of the ability of nanoceria particles to form such species upon reaction with atmospheric oxygen[33] was provided recently and cannot be ruled out in an aqueous environment. Thus the high reactivity of nanoceria particles leads to a huge number of possibilities for the particles to interact and scavenge ROS.

The mechanism of radical scavenging and auto-regeneration described above is a key distinction of nanoceria from other anti-inflammatory agents. Nanoceria may be a promising alternative for two main reasons: it has potential to reduce tissue damage without side effects, and it may curb the need for repeated dosing. Generation and proliferation of free radicals inside the body is caused by expression of pro-inflammatory enzymes such as iNOS. The iNOS protein can be activated by macrophages and other ROS to produce NO. Our data show that the treatment of J774A.1 cells with cerium oxide nanoparticles resulted in a distinct concentration-dependent suppression in the production of iNOS protein and mRNA levels in addition to decreasing ROS (Figures 3 and 4). This is similar to our previous findings that nanoceria prevented retinal degeneration in cell culture by inhibiting ROS. Reductions in ROS and inflammatory protein levels can be associated with a reduction in tissue damage caused by inflammation. These findings are noteworthy because mice given a twice-administered high (0.5 mg kg-1) dose of nanoceria did not experience any tissue damage up to at least 30 days post-administration (Figures 5 and 6). The other important feature of nanoceria is that repeated dosing may be unnecessary or reduced as we have observed the ability of

ceria to cycle between the 3+ and 4+ oxidation states. In our current studies, intravenously administered nanoceria particles remained deposited in tissues at least 30 days after injection, bolstering the lessened need for redosing. Although it was evident that iNOS protein levels were decreased and ROS production was abrogated in stimulated cells treated with nanoceria, one must be cautious when quenching ROS completely. Indeed, low levels of ROS are essential for normal cellular function and depleting ROS in non-stimulated cells may have pathologic consequences.

The results presented in the current research are unique from previous studies that report neuronal-, cardio-, and radiation-induced protective effects. Many of the mentioned studies show increased cell viability with nanoceria treatment, but few show direct ROS alleviation. One study reports descriptional inflammatory protein reductions as a result of nanoceria treatment,[18] yet we are the first to show the direct mechanism of ROS scavenging through iNOS protein reduction. The water-dispersed nanoceria particles used were completely characterized for particle size, oxidation state, and other properties unlike previously reported studies, which use commercial nanoceria. Characterization gives product consistency in size and shape, and assures the ability of nanoceria to switch between 3+ and 4+ oxidation states. Starting with a well-characterized water-based nanoceria solution is important because of the stability and consistency in concentration, two important characteristics to consider if nanoceria will one day be used as a clinical treatment. The current study also provides original evidence of cellular and tissue uptake with a cellular uptake mechanism.

We also recognize that it is important to look beyond the protective effects of nanoparticles, namely in reference to their toxicity. E. J. Park et al. recently reported a study of oxidative stress in cultured BEAS-2B cells as induced by nanoceria.[34] Using an

MTT assay, the authors reported decreases in cell viability in response to nanoceria treatment. Their findings do not warrant comparison to our studies for numerous reasons. Their lowest concentration at 10 ppm is six-fold that of our highest and the nanoceria used in their study was prepared differently (hydrothermally) and was not optimized for biocompatibility (larger in size and with sharp edges). Despite the high concentrations of non-optimized nanoceria, decreased cell viability was reported in only one of three cell types examined. Additionally, the recent paper by Andre Nel et al.[35] used well-characterized nanoceria and reported findings contradictory to Park et al. despite using larger nanoceria particles used in our studies. From our studies and the studies described above, we conclude that nanoceria is nontoxic at biologically relevant concentrations.

Lastly, other nanoparticles are currently under investigation due to their anti-inflammatory properties. Nanosilver is one of the more popular nanomaterials studied, however, its mechanism is mainly antibacterial.[36] New antibacterial drugs are important to decrease the emergence of resistant bacterial strains and should be used only when necessary. Nanosilver has also been reported to increase ROS.[36] We therefore have investigated nanoceria as a free-radical quencher to be potentially used as a treatment for inflammation only. We also focused our attention on cerium oxide as opposed to other nanoparticles because of its unique potential to self-regenerate. No other treatments have been suggested to have this capability, which could confer the beneficial side effect of decreased dosing.

CONCLUSION

Our studies give us confidence to continue the investigation of nanoceria as an antioxidant to decrease ROS production and inhibit inflammation in a biological model. We show that nanoceria decreases NO production in J774A.1 macrophages and is deposited in tissues of C57BLK6 mice following intravenous injections without overt pathology. Considering the immense array of diseases caused by inflammation, the ROS scavenging ability of nanoceria may have the potential to serve as a treatment for a broad spectrum of inflammatory diseases.

3.4. MATERIALS AND METHODS

3.4.1. Synthesis of ceria nanoparticles

Cerium oxide nanoparticles were synthesized using simple wet chemistry methods. In a typical synthesis, a stoichiometric amount of cerium nitrate hexahydrate (99.999% from Sigma-Aldrich) was added to 50 mL of deionized water (18.2 M) and stirred for 1 h. The cerium(III) ions in the solution were oxidized to cerium(IV) oxide and the pH of the solution was kept below 3.5 to maintain the synthesized ceria nanoparticles in suspension. Crystalline nanoparticles of cerium oxide form immediately upon oxidation.

3.4.2. UV-Vis spectrophotometry

The UV-Vis measurement was done using a Varian CaryOne spectrophotometer. A homogenous clear suspension of nanoceria (3 mL) was used to collect the spectrum. The UV-Vis spectrum was collected after aging the nanoparticles in solution for 7 days. A corresponding spectrum of cerium nitrate and cerium ammonium nitrate was also recorded to establish the relative positions of cerium(III) and cerium(IV) oxidation states in the spectrum.

3.4.3. XPS

High-resolution XPS measurements were done using a 5400 PHI ESCA (XPS) spectrometer using Mg K as source of X-rays operating at a power of 300W. The base pressure during the measurements was below 9-10 torr. Thin films of ceria as coatings were prepared by dip coating a glass slide. The slide was dried completely by vacuum drying and transported to the chamber in vacuum. The instrument was calibrated using a standard gold sample with the binding energy at 84.0 ± 0.1 eV. The charging shift produced in the spectrum was calibrated with the binding energy of carbon 1s (284.6) as baseline.

3.4.4. Cell culture and treatment

All cellular studies were conducted with a murine J774A.1 macrophage cell line (ATCC) incubated in culture using Dulbecco's modified Eagle medium (DMEM) 1 × media (Mediatech) supplemented with fetal bovine serum (FBS) (10%) (Hyclone) and penicillin/streptomycin (1%) (Mediatech). Cells were incubated at 37 °C with 5% CO2 and 95% air. For all experiments, cells were plated in 6-well plates at 2.5 × 105 cells mL-1. For nanoceria treatment or pretreatment, cells were incubated with the specified concentration of nanoceria in a fresh cell culture medium for 24 h. For cell stimulation, old medium was removed and replaced medium supplemented with lipopolysaccharide (LPS) (1 μL mL-1) (Sigma) and reconstituted IFN- (Accurate Chemical) (100 U mL-1). Cells were incubated for another 24 h.

3.4.5. HRTEM and SAED

HRTEM images of samples were obtained using a Zeiss 10 CA electron microscope. After treatment for 24 h with 10 μM nanoceria, cells were collected, fixed, and processed as previously reported.[37] Cells were then embedded in paraffin by an established

protocol[38] and examined at an energy of 60 keV. Cerium oxide nanoparticles were further identified using a FEI TECNAI F30 electron microscope (300kV) to obtain high magnification images and collect SAED patterns.

3.4.6. Flow cytometry

Cytotoxicity from nanoceria treatment was assessed by determining the levels of apoptosis and necrosis in treated cells using an Annexin-V/propidium iodide (PI) kit (Biovision). During apoptosis, phosphatidylserine (PS) molecules located in the cellular membrane translocate to the cell surface. Fluorescently-coupled Annexin-V attaches to PS on the outer membrane. PI is a fluorescent intercalating agent that binds to DNA and thus detects lysed and/or physically damaged cells. Macrophages were prepared as described in cell culture and treatment methods above. Cells in supernatant were collected and the remaining cells were detached and collected using trypsin-EDTA (MediaTech). Cells were immediately washed with bovine serum albumin (BSA) (1%) in PBS and resuspended in 1 × binding buffer with appropriate amounts of Annexin-V/PI and incubated at room temperature in darkness for 5 min. FITC/PI fluorescence was gated and apoptosis/necrosis levels were measured using flow cytometry.

3.4.7. Western blot

Cells were detached by scraping, washed in 1 mL PBS, and brought up in CelLytic cell lysis buffer (Sigma) (100 μL) with protease inhibitor cocktail (Sigma) (5 μL of 200-fold diluted). A Bradford assay was performed and equal amounts of protein were added to Laemmli buffer (Sigma) and separated in Tris-HEPES-SDS (10%, no gradient) precast polyacrylamide mini gels (Pierce). Protein expression levels were determined by incubating membranes in purified mouse anti-iNOS/NOS Type II antibodies (Transduction Laboratories) and then incubated with a secondary anti-mouse IgG HRP-

linked antibody (Cell Signaling). Protein levels were visualized using ECL Blotting Detection System (Amersham). Experiments shown are representative of four independent determinations.

3.4.8. Real-time RT-PCR

RNA was isolated from cell cultures using an RNeasy mini kit (Qiagen) and company protocol. Quality and concentration of RNA samples were detected using a Nanodrop Spectrophotometer and cDNA was generated using a high capacity cDNA reverse transcription kit (Applied Biosystems) with thermal cycling conditions run at 10 min at 25 °C, 120 min at 37 °C, and 5 s at 85 °C. Real-time PCR was run using a Taqman gene expression assay (Applied Biosystems). cDNA (100 ng) was loaded in triplicate with Taqman mastermix and probes and PCR was run on an iCycler IQ machine at 95 °C for 10 min followed by 40 cycles of 15 s at 95 °C and 1 min at 60 °C. Messenger RNA levels were determined relative to the housekeeping gene hprt1 and fold differences within each group were calculated.

3.4.9. Microplate detection system

Intracellular superoxide levels were detected using a Diogenes cellular luminescence enhancement system (National Diagnostics). The Diogenes kit is a super-sensitive version of the traditional luminol assay to measure oxidation levels that are directly proportional to chemiluminescence. Cells were pretreated and stimulated according to cell treatment methods listed above. Cells were collected by scraping, washed once with PBS, counted and plated in a 96-well plate a (2 × 105 cells in 50 µL). An equal volume of Diogenes reagent was added and luminescence levels were measured at 1 min intervals during a 30 min time period at 37 °C with a Safire 2 microplate reader. Results shown are

representative of three independent experiments. Averages of 5 min each were taken and plotted over time to correct for variability and sensitivity of the assay.

3.4.10. Confocal microscopy

ROS levels were measured using DCF fluorescence. After a pretreatment (10 μM) and stimulation described above, DCF-diacetate (DCF-DA) (Sigma) dissolved in dimethyl sulfoxide (DMSO) was added in staggered additions to the cells (20 μM final concentration) in PBS supplemented with FBS (2%). Cells were incubated in solution for 20 min at 37 °C, during which the DCF-DA molecules that entered the cells are cleaved by esterases to non-fluorescent DCF-H, and are thereafter cleaved by ROS to fluorescent DCF. Five random images of each sample were obtained and fluorescence visualized (excitation 488 nm, emission 515-555) under identical parameters for each sample.

3.4.11. Histopathology

Eight C57BL/6 mice were injected intravenously on day 1 with nanoceria (0.1 mg kg-1, low dose) suspended in 100 μL of PBS and a second group of eight mice were injected with a high dose of nanoceria (0.5 mg kg-1). Eight control mice were injected with PBS. Four mice of each group (high dose, low dose, and control) were euthanized 7 days post administration, necropsied, and major organs were harvested and processed for histopathology. Sections of tail, kidney, and liver were saved for ultrastructural examination. On day 15, the remaining experimental mice received a repeat administration of high or low dose ceria and control mice received PBS. Thirty days post initial administration, all remaining mice were euthanized, necropsied, and histopathology and ultrastructural examination of major organs performed. TEM was performed using a Zeiss 10 CA electron microscope run at 60 keV to examine the tail site of injection, liver, and kidney. Images shown are representative of 4 independent trials.

The institutional committee at Virginia Tech approved all animal experiments (Animal Welfare Assurance # iA-3208-01;expires 3-31-2010; IACUC protocol # 05-092-CMV).

3.4.12. Statistical analysis of data

Data are presented as mean ± standard error of mean (SEM). Annexin V and ROS data were analyzed using two-way ANOVA. Real-time data was analyzed using one-way ANOVA with Tukey's post analysis. A p value 0.05 was considered significant.

ACKNOWLEDGEMENTS

Dr. Reilly acknowledges Beverly Rzigalinski, Ph.D. for her assistance in the initial phases of the project, her insightful comments, and her assistance in obtaining extramural funding for the project. This work was funded by the Arthritis Foundation and the National Institute of Health (1 R15 AI072756-01A2).

3.5. LITERATURE CITED

[1] V. K. Singh, S. Mehrotra, P. Narayan, C. M. Pandey, S. S. Agarwal, *Immunol Res* **2000**, *22*, 1.
[2] I. Sabroe, L. C. Parker, P. M. Calverley, S. K. Dower, M. K. Whyte, *Postgrad Med J* **2008**, *84*, 259.
[3] H. Ahsan, A. Ali, R. Ali, *Clin Exp Immunol* **2003**, *131*, 398.
[4] A. H. Tremoulet, S. Albani, *Expert Opin Investig Drugs* **2006**, *15*, 1427.
[5] P. Amiri, R. M. Locksley, T. G. Parslow, M. Sadick, E. Rector, D. Ritter, J. H. McKerrow, *Nature* **1992**, *356*, 604.
[6] S. R. Tsunekawa S, Ohsuna T, Kasuya A, Takahashi H, Tohji K., *Mater Sci Forum* **1999**, 315.
[7] M. Das, S. Patil, N. Bhargava, J. F. Kang, L. M. Riedel, S. Seal, J. J. Hickman, *Biomaterials* **2007**, *28*, 1918.
[8] J. C. Yu, L. Zhang, J. Lin, *J Colloid Interface Sci* **2003**, *260*, 240.
[9] C. Korsvik, S. Patil, S. Seal, W. T. Self, *Chem Commun (Camb)* **2007**, 1056.
[10] J. Chen, S. Patil, S. Seal, J. F. McGinnis, *Nat Nanotechnol* **2006**, *1*, 142.
[11] J. Chen, S. Patil, S. Seal, J. F. McGinnis, *Adv Exp Med Biol* **2008**, *613*, 53.
[12] R. W. Tarnuzzer, J. Colon, S. Patil, S. Seal, *Nano Lett* **2005**, *5*, 2573.
[13] M. F. Hochella, Jr., S. K. Lower, P. A. Maurice, R. L. Penn, N. Sahai, D. L. Sparks, B. S. Twining, *Science* **2008**, *319*, 1631.

[14] M. Nolan, S. C. Parker, G. W. Watson, *Phys Chem Chem Phys* **2006**, *8*, 216.
[15] M. Nolan, S. C. Parker, G. W. Watson, *J Phys Chem B Condens Matter Mater Surf Interfaces Biophys* **2006**, *110*, 2256.
[16] B. A. Rzigalinski, K. Meehan, R. M. Davis, Y. Xu, W. C. Miles, C. A. Cohen, *Nanomed* **2006**, *1*, 399.
[17] B. A. Rzigalinski, *Technol Cancer Res Treat* **2005**, *4*, 651.
[18] J. Niu, A. Azfer, L. M. Rogers, X. Wang, P. E. Kolattukudy, *Cardiovasc Res* **2007**, *73*, 549.
[19] Z. Markovic, V. Trajkovic, *Biomaterials* **2008**, *29*, 3561.
[20] O. I. Shadyro, I. L. Yurkova, M. A. Kisel, *Int J Radiat Biol* **2002**, *78*, 211.
[21] S. Patil, A. Sandberg, E. Heckert, W. Self, S. Seal, *Biomaterials* **2007**, *28*, 4600.
[22] K. Nakamura, S. Yamagishi, T. Matsui, T. Yoshida, K. Takenaka, Y. Jinnouchi, Y. Yoshida, S. Ueda, H. Adachi, T. Imaizumi, *Am J Pathol* **2007**, *170*, 2159.
[23] C. Bogdan, *Nat Immunol* **2001**, *2*, 907.
[24] A. Nel, T. Xia, L. Madler, N. Li, *Science* **2006**, *311*, 622.
[25] M. A. Balboa, J. Balsinde, *Biochim Biophys Acta* **2006**, *1761*, 385.
[26] C. Bertram, R. Hass, *Biol Chem* **2008**, *389*, 211.
[27] D. G. Olmedo, D. R. Tasat, P. Evelson, M. B. Guglielmotti, R. L. Cabrini, *J Biomed Mater Res A* **2008**, *84*, 1087.
[28] T. X. Sayle, S. C. Parker, D. C. Sayle, *Phys Chem Chem Phys* **2005**, *7*, 2936.
[29] E. G. Heckert, A. S. Karakoti, S. Seal, W. T. Self, *Biomaterials* **2008**, *29*, 2705.
[30] F. H. Scholes, C. Soste, A. E. Hughes, S. G. Hardin, P. R. Curtis, *Applied Surface Science* **2006**, *253*, 1770.
[31] F. H. Scholes, A. E. Hughes, S. G. Hardin, P. Lynch, P. R. Miller, *American Chemical Society* **2007**, *19*, 2321.
[32] B. Djuricic, S. Pickerinb, *Journal of the European Ceramic Society* **1999**, *19*, 1925.
[33] J. Guzman, S. Carrettin, A. Corma, *J Am Chem Soc* **2005**, *127*, 3286.
[34] E. J. Park, J. Choi, Y. K. Park, K. Park, *Toxicology* **2008**, *245*, 90.
[35] T. Xia, M. Kovochich, M. Liong, L. Madler, B. Gilbert, H. Shi, J. I. Yeh, J. I. Zink, A. E. Nel, *ACS Nano* **2008**, *2*, 2121.
[36] H. J. Park, J. Y. Kim, J. Kim, J. H. Lee, J. S. Hahn, M. B. Gu, J. Yoon, *Water Res* **2009**, *43*, 1027.
[37] *Poly/Bed 812 Data Sheet*, PolySciences, Inc.
[38] M. J. Dykstra, L. E. Reuss, *Microscopy: Theory, Techniques, and Troubleshooting* **2003**, *2*, 109.

Chapter 4

Bio-distribution and *In Vivo* Antioxidant Properties of Cerium Oxide Nanoparticles

ABSTRACT

Cerium oxide nanoparticles have oxygen defects in their lattice structure that enable them to scavenge oxygen radicals. The goal of our study was to perform a comprehensive analysis of the biological distribution and *in vivo* antioxidant capabilities of nanoceria administered mice. We examined peroral (PO), intravenous (IV), and intraperitoneal (IP) administration routes, biodistribution, clearance, histopathology and WBC counts to determine target organs and immunologic response to nanoceria. Next we examined if nanoceria administration would decrease ROS production in mice treated with carbon tetrachloride (CCl_4). Our results showed that the most extensive and cumulative nano-deposition in IV and IP administered mice, while PO mice excreted greater than 95% of their doses. As determined by ICP-MS, nanoceria organ deposition for IV and IP mice was greatest in the spleen followed by the liver, lungs, and kidneys. Elimination for all administration routes was through feces. Nanoceria distribution was confirmed with IVIS in vivo imaging, and deposition was confirmed with TEM. There was no statistical difference in histopathology grades between control and nanoceria dosed mice, however, nanoceria dosed mice generally showed elevated WBC counts. IV nanoceria treatment appeared to reduce markers of oxidative stress in mice treated with carbon tetrachloride (CCl_4) to induce ROS production. Taken together, our data suggest that nanoceria treatment has the potential to reduce oxidative stress.

4.1 INTRODUCTION

Inflammation is the body's complex and highly regulated response to stimuli such as physical damage, pathogens, or irritants.[1] Free radicals and reactive oxygen species (ROS) are often produced during inflammatory cascades. ROS have been reported to play a role in the maintenance of cell homeostasis and protective functions during acute inflammation.[2] However, when an imbalance between ROS production and elimination occurs, cells and tissues experience oxidative stress.[2] Although the precise etiology of persistently abundant ROS levels remains unknown, ROS overproduction has been linked with numerous chronic inflammatory and autoimmune diseases including atherosclerosis, rheumatoid arthritis, diabetes, multiple sclerosis, and others.[2]

ROS are defined as molecules with one or more unpaired electrons in their outer orbital. Due to the presence of unpaired electrons, these molecules are highly unstable and tend to react with adjacent molecules, stripping them of electrons and consequently altering their structure and function. Free radical species produced within the cell include superoxide (O_2^-), the hydroxyl radical (•OH), NO, peroxynitrite ($ONOO^-$), lipid hydroperoxides, and others.[3] In hydrophobic areas such as the plasma membrane, ROS can cause chain reactions in which an unpaired electron is passed from fatty acid to fatty acid, generating multiple free radical species, widespread damage, and ultimately cell death.[4-6]

The body has various enzymatic and non-enzymatic antioxidants it can generate or consume respectively to deactivate free radicals and ROS.[7] Non-enzymatic antioxidant supplements and diets rich in antioxidants are a form of treatment for sufferers of oxidative stress.[8] Tocopherols (vitamin E), carotenes, oxy-carotenoids,

vitamin A, ubiquinols, ascorbate (vitamin C), glutathione, and other antioxidants combat plasma membrane, fatty acid, protein, and DNA oxidative damage.[9] While these antioxidants are critical for cellular homeostasis, it is important to note that non-enzymatic antioxidants must be continually replenished, and that the body may not always be able to generate enough enzymatic antioxidants to restore a healthy balance.[9, 10]

N-Acetyl Cysteine (NAC) is a widely used antioxidant, most often used to protect the liver from oxidative damage caused by ROS. It is administered orally or intravenously and is commonly used to treat acetaminophen poisoning in humans.[11, 12] NAC is an acylated (to infer water solubility) version of the amino acid L-cysteine. Cysteine is the limiting amino acid used in the production of the antioxidant glutathione (GSH), which needs only three amino acids to function: glutamic acid, cysteine, and glycine.[13] GSH is the predominant anti-oxidant in the aqueous cytoplasm of cells, and its production is primarily in the lungs and liver.[13] In addition to its antioxidant activity, NAC has also been shown to inhibit the pro-inflammatory NFκ-B transcription factor.[14] However, NAC has a half-life of about 5 hours and when used to treat acute oxidative stress must be continually replenished and is not practical for the treatment of chronic oxidative stress.

Cerium oxide nanoparticles (nanoceria) have a unique electronic structure due mainly to its large surface-area-to-volume ratio that creates oxygen defects.[15, 16] It is these defects, or reactive sites on the nanoceria surface that act as sites for free radical scavenging and are currently being investigated as therapeutic interventions in biological systems.[3, 17, 18] It has recently been reported that cerium oxide can act as a catalyst that mimics the antioxidant enzyme superoxide dismutase.[19] Additionally, the ability of

engineered cerium oxide nanoparticles to confer neuronal,[20] ocular,[21, 22] and radioprotection[6] has been demonstrated. This versatile biomaterial has the potential to be used in nanotherapeutics to decrease mediators of chronic inflammation without repeated dosings. We previously demonstrated the *in vitro* ROS scavenging actions of nanoceria in J774A.1 macrophages and their successful uptake *in vivo*. Here we report an *in vivo* bio-distribution study detailing organ distribution, cellular uptake, immune response to, and anti-inflammatory effects of nanoceria administration. Unlike other studies that have investigated nanoceria's ability to reduce tissue damage, we examined the direct effect of nanoceria to decrease oxidative metabolite levels in mice experiencing oxidative stress.

4.2 RESULTS

4.2.1. *In vitro* antioxidant properties of nanoceria.

We have previously reported the ROS scavenging abilities of nanoceria in J774A.1 macrophages.[23] We found that nanoceria pretreatment decreases protein and mRNA levels of inducible nitric oxide synthase (iNOS), an enzyme that produces the ROS nitric oxide (NO). We further examined nanoceria's ability to reduce NO in our current studies. We performed a Greiss assay to assess nitrate (NO_3^-) levels in nanoceria pretreated, lipopolysaccharide (LPS) and interferon gamma (IFN-γ) stimulated macrophages. Nitrates are byproducts of the oxidation of cellular macromolecules by NO. Nanoceria was dialyzed to reduce residual nitrates in the nanoceria solution in order to reduce interference with the assay. We found a dose dependent decrease of nitrates with a significant reduction occurring around the 10 μM dose and a near return to control levels around the 20 and 30 μM doses **(Figure 4.1).** We found no differences in NO levels in nanoceria pretreated, non-stimulated macrophages (results not shown). Our

results further exemplify nanoceria's ability to scavenge NO, a ROS that plays a critical role in numerous chronic inflammatory diseases.

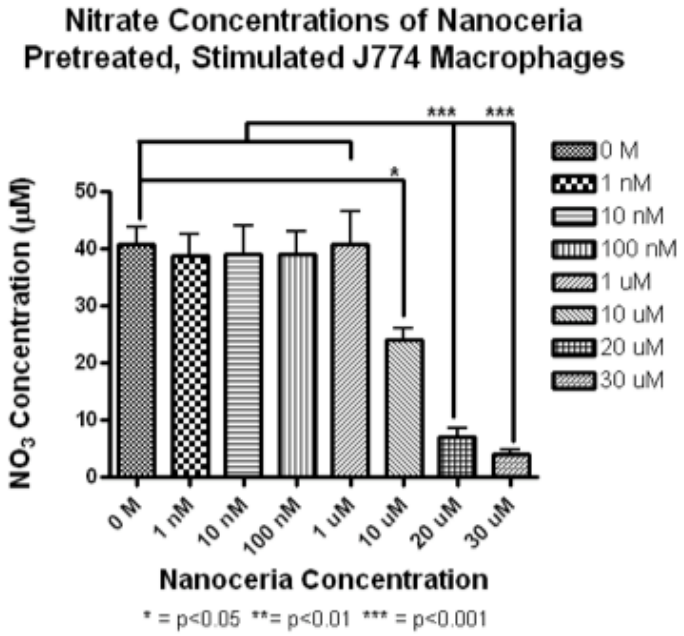

Figure 4.1. Greiss assay to determine nitrate levels of J774A.1 macrophages. Cells were pretreated for 24 hours in varying concentrations of nanoceria and then stimulated with LPS and IFN-γ for 16 hours. A dose dependent decrease in nitrate levels was observed in nanoceria pretreated macrophages. A significant decrease occurred around the 10 μM concentration and nitrate levels returned to near control levels around 20 and 30 μM. Nitrate levels of pretreated, non-stimulated cells did not show any observable effects. Data was analyzed using a one-way ANOVA in GraphPad and an $n \geq 3$ was used with a $p < 0.05$ being considered significant.

4.2.2. Determining the *in vivo* nanoceria administration route: bio-distribution and histopathology

We first sought to determine nanoceria deposition and clearance using different administration routes. Ten week-old, CD1, female mice were administered nanoceria at a previously determined concentration (0.5 mg/kg) through either the peroral (PO), intravenous (IV), or intraperitoneal (IP) routes. Control mice were administered

phosphate buffered saline (PBS) by the same route. The study was duplicated in mice receiving either 2 or 5 sets of injections in order to examine saturation of the system. Using inductively coupled plasma mass spectrometry (ICP-MS), we determined nanoceria deposition and clearance.

We found that IV administration resulted in the greatest deposition, followed by the IP and PO routes **(Figure 4.2)**. In both IV and IP administered mice, the spleen had the highest concentration of nanoceria as measured in micrograms of nanoceria per gram of tissue, followed closely by the liver. The lungs and kidneys also showed deposited nanoceria, but at very minimal concentrations. PO administered mice had negligible nanoceria deposition in any organ except for very low concentrations detected in the lungs. Clearance of nanoceria through feces was greatest (~98%) in PO mice, followed by IP and IV mice. There was no detectable nanoceria in the urine of any group. Similar results were found in both the two and five-week studies, with nanoceria deposition concentrations being about 3 times higher in the 5-week group (that received 3 more injections) than in the 2 week group (2 week data not shown). These results show that systems do not reach saturation two weeks after administrations at the concentration we used, and that very little nanoceria was cleared from organs throughout the time period of the study.

In addition to determining biodistribution, we also sought to determine if nanoceria deposition in major organs would result in pathologic findings. This was determined by examining hematoxylin and eosin (H&E) stained tissue sections of all major organs. Sections were scored on a scale from 0 to 4, based on severity of pathologic changes (0 = unremarkable, 1 = minimal changes, <5% of organ affected, 2 = mild, 5–15% of organ affected, 3 = moderate, 16–40% of organ affected, 4 = marked,

>40% of organ affected). We found a lesion in the spleen of an IP control mouse, a reactive Peyer's patch in the small intestine of an IP ceria mouse, and a pulmonary hemorrhage in an IV ceria mouse. Both control and experimental groups kidney scores greater than 0 were common, however when averaged and compared, no significant differences between scores of any group were found **(Figure 4.2).** Our findings indicate that nanoceria administration did not cause overt pathology in any group and that the routes of administration did not affect toxicology or pathology. Due to the highest deposition and lack of pathogenicity, we determined that IV administration of ceria was the optimal route for tissue accumulation.

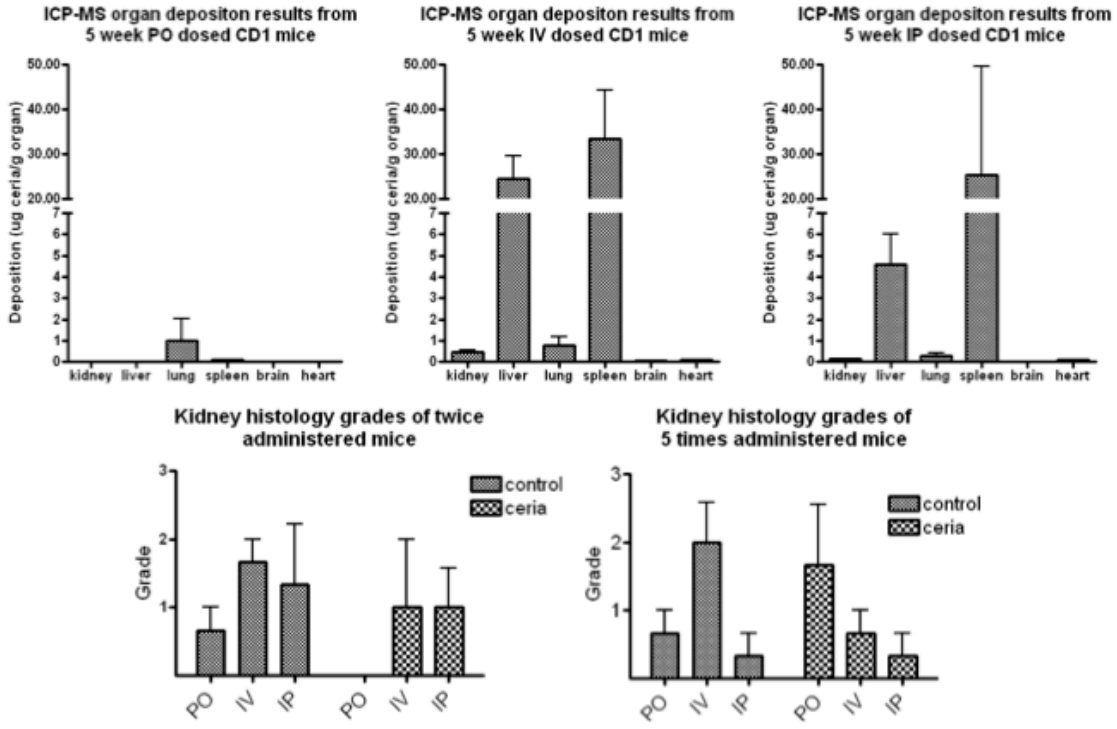

Figure 4.2 Biodistribution and histopathology of nanoceria administered CD1 mice. Mice were administered nanoceria at 0.5 mg/kg via peroral (PO), intravenous (IV), or intraperitoneal (IP) routes. Control mice were administered PBS. Administrations were once a week for either 2 or 5 weeks. Major organs were collected a week after last nanoceria administration and were evaluated for cerium deposition concentrations using inductively coupled plasma mass spectrometry (ICP-MS). Spleens showed the greatest deposition followed closely by the liver. Lungs, kidneys and hearts showed minimal

deposition, while there were no detectable cerium levels in the brain. Data of 2-week administration not shown as it shows the same trend but with levels about 3 times less than that of the 5-week data. Histology grades were assigned to H&E stained tissues of all mice; higher grades correspond to greater pathologies. There were no consistent pathologies noted except for in the kidneys, however, results were found in both control and experimental groups.

4.2.2. Immune response of CD1 mice to nanoceria.

While histopathology showed that nanoceria administration had no toxic findings in CD1 mice, we further investigated the immune response of mice to nanoceria by manually measuring total white blood cell (WBC) counts. Heparinized (anticoagulated) blood from mice was collected, red blood cells were lysed, and WBC counts were performed 4 times for each sample and averaged for a final count. WBC counts between control and nanoceria dosed mice in the 2-week study showed minimal differences; however, levels generally increased in mice in the 5-week study **(Figure 4.3)**. While WBC levels naturally increase with age, the counts were somewhat higher in mice given nanoceria as compared to controls, with the exception of IP administered nanoceria.

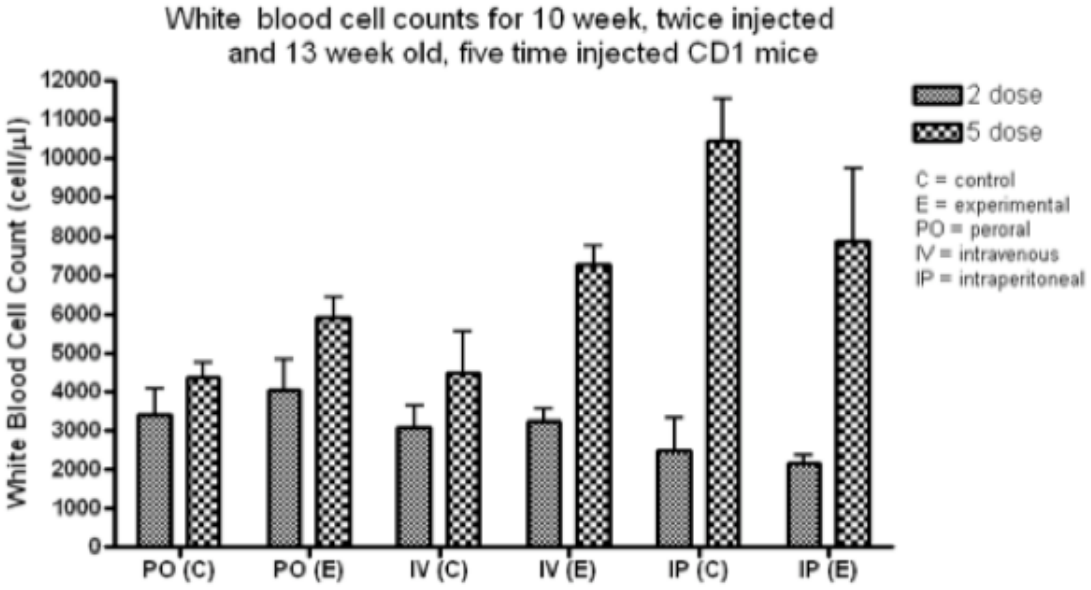

Figure 4.3 Immune response of nanoceria administered CD1 mice. Mice were administered nanoceria at 0.5 mg/kg via peroral (PO), intravenous (IV), or intraperitoneal

(IP) routes. Control mice were administered PBS. Administrations were once a week for either 2 or 5 weeks. Blood was collected immediately before euthanization one week after the last administration and analyzed for white blood cell (WBC) levels. WBC levels do not appear to be different between control and 2-week administered mice, however levels are generally elevated between control and 5-week administered mice. Immune responses in both control and nanoceria administered mice were greater in IP followed by IV and PO routes.

4.2.3. Real-time biodistribution and cellular uptake mechanism of nanoceria administered CD1 mice.

While measurements using ICP-MS helped us determine nanoceria deposition in larger organs, we employed other techniques to look for the deposition of nanoceria in organs too small to measure with ICP-MS and to examine the mechanism of cellular uptake. Using an IVIS real-time imaging station, we visualized the presence of fluorescently tagged nanoceria in mice 2 hours post IV injection **(Figure 4.4).** In addition to fluorescence corresponding to the liver, spleen, and lungs, deposition also appeared in small, peripheral areas around the neck and axilla, possibly corresponding to lymph nodes. We also used transmission electron microscopy (TEM) to examine each organ of nanoceria administered mice to look for localized deposition. Nanoceria appears as small, dense, black structures in TEM images. We found numerous nanoceria suspect particles in clusters of lysosomes in the kidneys **(Figure 4.4).** This is likely an accurate finding as lysosomes are responsible for collecting and digesting foreign materials in the body. Nanoceria could not be located in other organs due to the similarity of nanoceria to agglomerates of iron in heme from red blood cells.

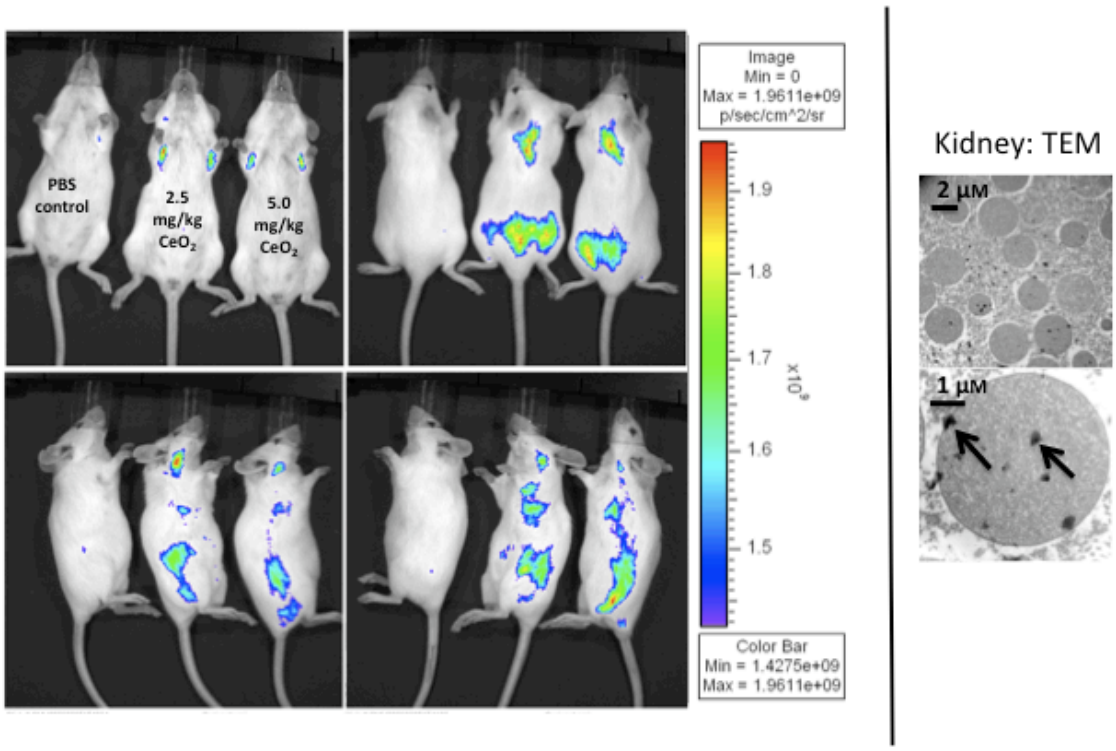

Figure 4.4 Real-time biodistribution and cellular uptake of nanoceria administered CD1 mice. Mice were IV administered either 2.5 (middle) or 5.0 (right) mg/kg of FAM-tagged nanoceria. Control mice (left) were given PBS. Mice were sedated with a continual flow of IsoFlow™ and nanoparticles were viewed 2 hours after injection using an IVIS imaging station with an excitation of 385 nm, emission of 509 nm, using an f-stop of 4 with 2-second exposures. Nanoceria appeared deposited in organs corresponding to those determined earlier in addition to areas in the axilla and neck, possibly corresponding to lymph nodes. HRTEM was performed on all major organs. There were numerous nanoceria suspect particles in clusters of lysosomes in the kidneys. Nanoceria could not be located in other organs due to the similarity of nanoceria to agglomerates of iron in heme from red blood cells.

4.2.4. *In vivo* antioxidant properties of nanoceria. We next sought to determine if nanoceria would extend antioxidant effects in an animal model. To induce ROS production, we injected carbon tetrachloride (CCl_4) intraperitoneally, which has been shown to induce liver toxicity and oxidative stress.[24] Prior to CCl_4 injections, we administered nanoceria IV at 0.05 mg kg-1. In addition, we administered the antioxidant N-acetyl cysteine (NAC) to a second group of mice as a comparison. NAC has been shown to decrease ROS production in mice administered CCl_4. In humans it has been

used therapeutically as an antioxidant in individuals suffering acute liver toxicity. NAC has a half-life of around five hours and therefore needs to be administered hourly to maintain its effectiveness. Negative control mice were given PBS only. An experimental timeline is outlined in Figure 5. Thirty mice in groups of 10 were administered PBS, nanoceria, or NAC on weeks 1 and 2. On week 2, half of the mice (5) in each group of 10 were given IP CCl_4 2 hours after their initial injections as an inducer of liver toxicity. The other half were given PBS IP injections. Blood and urine were collected on week 2. On week 3, mice received repeat CCl_4 or PBS IP injections. Blood, urine, and livers were then collected for analysis. Oxidative damage to DNA was measured with 8-hydroxydeoxyguanosine (8-OHdG) levels in urine, and lipid peroxidation was measured by 8-isoprostane (8-iso) levels in livers and malondialdehyde (MDA) in plasma.

Week 1	Week 2		Week 3
Group 1: 10 mice IV PBS	Group 1: 10 mice IV PBS	5 mice IP CCl_4	5 mice IP CCl_4
		5 mice IP PBS	5 mice IP PBS
Group 2: 10 mice IV CeO_2	Group 2: 10 mice IV CeO_2	5 mice IP CCl_4	5 mice IP CCl_4
		5 mice IP PBS	5 mice IP PBS
Group 3: 10 mice PO NAC	Group 3: 10 mice PO NAC	5 mice IP CCl_4	5 mice IP CCl_4
		5 mice IP PBS	5 mice IP PBS
	Urine collection and blood draw		Urine collection, blood draw, livers removed

4.5 Outline of BALB/c mouse experiment.

Urine in each group was collected for seven hours post IP injections and was pooled and assessed for ROS production by determining 8-OH-dG levels. In mice

stimulated with CCl_4 in week 2, our results showed a decrease in 8-OH-dG levels in mice preadministered with both nanoceria and NAC, while PBS treated groups maintained higher levels of 8-OH-dG **(Figure 4.6).** In the same group of mice on week 3 in which there was no pre-administration of drugs, there a slight increase in 8-OH-dG levels observed in the nanoceria and NAC groups compared to the PBS group. This suggests that nanoceria and NAC both decrease oxidative stress when administered immediately before ROS production. In negative control groups on weeks 2 and 3 in which oxidative stress was not stimulated (PBS IP injections), we observed a slight increase in 8-OH-dG levels with nanoceria and NAC administration compared to PBS. Overall, however, CCl_4 treated groups did not display significantly higher levels of DNA oxidative damage than PBS treated groups and therefore oxidative stress was not stimulated and it cannot yet be determined whether nanoceria treatment reduces ROS during oxidative stress.

MDA levels indicative of lipoperoxidation were measured in blood drawn from mice 3 hours post IP injections. Significant decreases were observed in nanoceria treated mice in the CCl_4 injected groups in both weeks 2 and 3, however the lack of oxidative stress stimulation in CCl_4 groups again prevents us from drawing solid conclusions about nanoceria antioxidant behavior from our observations **(Figure 4.6).**

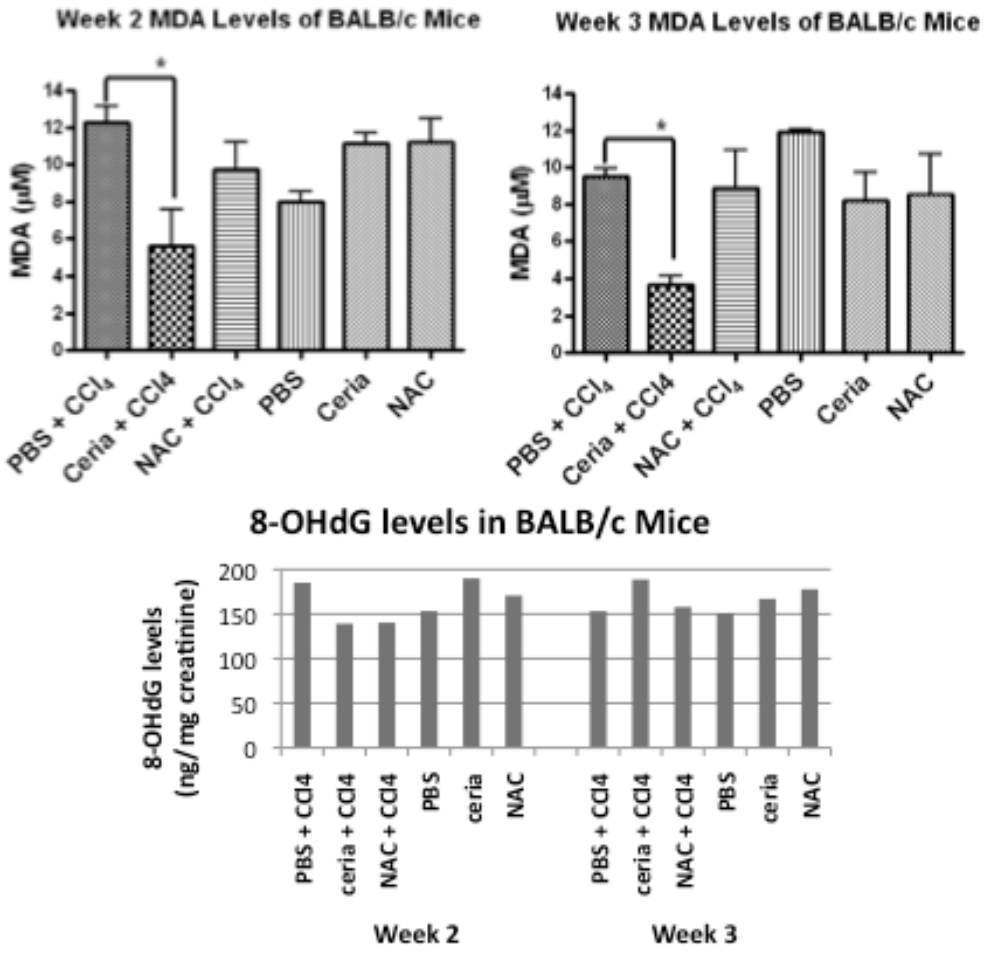

Figure 4.6 Measuring markers of oxidative stress in nanoceria administered mice. Different markers of oxidative stress were measured in ROS induced (using CCl_4) BALB/c mice injected with nanoceria or N-acetyl cysteine, a commonly administered antioxidant. Consistent decreases in plasma MDA levels and urinary 8-OH-dG were observed in nanoceria administered mice on week 2 of the experiment as opposed to week 3. Basal oxidative stress markers were also elevated in mice administered nanoceria that did not receive CCl_4. Solid conclusions cannot be drawn from data due to lack of ROS production stimulated by CCl_4. Data were analyzed using a one-way ANOVA and each group shares an n of 5.

4.3 DISCUSSION AND CONCLUSION

ROS are key mediators of inflammation whose role is to oxidize and thereby damage surrounding macromolecules. ROS oxidize proteins, DNA, and lipids, often initiating chain reactions in which consecutive structures are damaged as electrons are

repeatedly lost and stripped from neighboring molecules.[2, 25] Oxidation can cause loss of lipid or protein structure, leading to a loss of function and cell death. Oxidized DNA can lead to mutations and altered phenotype if not repaired.[25] While ROS has a protective mechanism against foreign invaders and disease, ROS act indiscriminately and cells experience oxidative stress when an imbalance between ROS production and elimination occurs.[2] The precise etiology of persistently abundant ROS levels remains unknown, yet oxidative stress has been linked with numerous chronic inflammatory and autoimmune diseases.[2] Quenching ROS production and oxidative damage can decrease inflammation and subsequent tissue injury and death. In our current studies, our goal was to investigate the ability of nanoceria to decrease markers of oxidative stress in mice with induced liver toxicity. We began by expanding upon our previous findings that nanoceria reduces ROS *in vitro* in J774A.1 macrophages. The optimal *in vivo* administration route through which to deliver nanoceria in mice was then determined in addition to observing biodistribution, histopathology, and cellular uptake mechanisms.

The functionality of cerium oxide nanoparticles lies in their ability to reversibly switch between the 3+ and 4+ oxidation states. The regenerative antioxidant properties are due, in part, to the valence structure of the cerium atom combined with inherent defects in the crystal lattice and oxygen defect structure.[16, 18] Ceria nanoparticles undergo easy, fast, reversible reduction to substoichiometric phases and can readily take up and release oxygen, alternating between CeO_2 and CeO_{2-x}.[20, 26] Analysis of cerium oxide nanoparticles in previous studies[27] has shown that maximizing the 3+ oxidation state in nanoceria is imperative to its radical scavenging ability. In our studies, nanoceria was engineered to have both 3+ and 4+ oxidation states by ensuring a smaller particle size and thus higher concentration of defects as previously described.[23] Cerium oxide,

with its large number of defects and ability to couple in a redox manner, can quench free radicals with relative ease. Given the surface chemistry of nanoceria, there also appears to be evidence for regenerative action in situ.[18, 20, 27] The reversibility of the oxidation states at relatively lower oxidation potentials renders regenerative properties to nanoceria. The possible reactions involving the radical quenching and regeneration of oxidation states are:

(1) $Ce^{3+} + \bullet O_2^- + 2H^+(aq) \rightarrow Ce^{4+} + H_2O_2$ and

(2) $2Ce^{4+} + H_2O_2 \rightarrow 2Ce^{3+} + 2H^+ + \bullet O_2$

Surface oxygen vacancies expose the reduced and more active cerium(III) surrounded by a pool of cerium(IV) on the surface of nanoceria particle[27] and act as reactive sites for the free radicals where electron transfer from or to the ceria nanoparticles can occur. It can also be hypothesized that immobile oxygen vacancies on the surface provide binding sites for the superoxide and peroxide species to facilitate the electron transfer processes. Redox coupling can regenerate these reactive sites so that a single ceria nanoparticle has multiple defect sites and is sufficient to quench multiple radical species. All aqueous reactions at the surface are governed by surface potential and total redox potential and thus there are many more possibilities for ceria to scavenge nearby reactive species. It must be noted that the above equations do not represent the only mechanisms by which cerium in ceria nanoparticles may react with superoxide and hydroxyl radicals. Recent investigations also suggest that cerium ions can react with peroxide type radicals to form an intermediate peroxo-complex.[28-30] While there is no direct evidence of the formation of this peroxo-complex upon reaction of peroxide with ceria nanoparticles, spectroscopic evidence of the ability of nanoceria particles to form such species upon reaction with atmospheric oxygen[30] was provided recently and cannot be ruled out in an aqueous

environment. Thus the high reactivity of nanoceria particles leads to a huge number of possibilities for the particles to interact and scavenge ROS.

We have previously reported nanoceria's ability to safely quench ROS *in vitro* in immune stimulated macrophages. Our current goal was to test the ability of nanoceria to relieve oxidative stress *in vivo* and compare our results to a known antioxidant, NAC. We used an inbred strain of BALB/c mice and induced hepatotoxicity, or chemical-driven liver damage, using carbon tetrachloride (CCl_4) to induce ROS production. CCl_4 has been well known to induce liver toxicity and over the years has been used in numerous experiments, including many oxidative stress studies.[24, 31, 32] CCl_4 has been shown to induce oxidative stress and its markers in rats and mice.[24] Three well-established markers include 8-isoprostane (8-*iso* $PGF_{2\alpha}$), 8-hydroxy-2-deoxy Guanosine (8-OH-dG), and Thiobarbituric Acid Reactive Substances (TBARS).[24, 33] 8-isoprostane is a lipoperoxidation metabolite formed by the random oxidation of tissue phospholipids by oxygen radicals. It is found under normal conditions, but is elevated during periods of antioxidant deficiency and oxidative stress. It is one of few isoprostanes with biological activity and causes renal and pulmonary vasoconstriction.[24] 8-OH-dG is another established marker of oxidative stress; specifically it is a metabolite of DNA damage. Free (not incorporated in DNA) nucleosides of hydroxylated guanosine is readily filtered by the kidneys and excreted in urine.[24] TBARS levels correspond to malondialdehyde (MDA) levels of lipid peroxidation in cells and tissues. MDA reacts with thiobarbituric acid (TBA) to form an MDA-TBA adduct easily measured using colorimetric or fluorimetric assays.[33] TBARS assays have been widely employed to measure oxidative stress, however, controversy surrounding the specificity of TBARS to compounds other than MDA has arisen. We still chose to employ this technique due to the volume

restrictions of our plasma samples, as large quantities of blood cannot be obtained from mice. Oxidative stress markers of these three types were compared among control, nanoceria, and NAC administered mice. NAC was used as a comparative antioxidant because it is a widely used treatment for oxidative stress, namely liver toxicity. It is most often used to treat acetaminophen poisoning but must be administered in a high one-time dose followed by smaller hourly doses due to its short half-life of about 5 hours.[12, 13] NAC is an effective treatment under strictly acute conditions, however it would not be effective in the treatment of chronic oxidative stress. We have shown nanoceria, on the other hand, to remain deposited in the liver and spleen for a period of at least 30 days. This property, in addition to the regenerative nature of cerium oxide nanoparticles, would make nanoceria a much more effective, manageable antioxidant treatment for chronic oxidative stress.

We recognize the importance of investigating the biocompatibility of nanoceria in our research. We show the biodistribution of nanoceria mainly in the spleen and liver, with trace amounts in the lungs and kidneys, and virtually none in the heart or brain. The spleen is one of the most vascular organs in the body, whose responsibilities, in part, include recycling red blood cells and playing a major role in the immune system. It is highly probable that either macrophages carry foreign bodies (including nanoceria) to the spleen, or that the spleen takes in elevated concentrations of nanoceria due to the high numbers of resident macrophages. In all likelihood, both of these mechanisms should occur because we have already seen the ability of macrophages to engulf nanoceria and because elevated WBC counts were typically found in nanoceria administered mice. Macrophages, a type of WBC, would probably transport nanoceria to the spleen. The liver is another highly vascular organ with a major protective function of detoxification in

the body. Nanoceria deposition in the liver could be due to the presence of high numbers of Kupffer cells (resident macrophages) and/or the detoxification role. The kidneys, lungs, and the heart are the remaining major organs that retained very low concentrations of nanoceria, despite their high vascularity. Due to the fact that the spleen and liver had the highest nanoceria deposition concentrations than other organs in the body and because WBC counts were higher in nanoceria administered mice, it is probable that immune recognition accounts for the distribution of nanoceria in these organs. It is important to note that nanoceria did not cross the blood brain barrier (BBB).

The lack of nanoceria accumulation in the kidneys or excretion in urine was unexpected. We would have expected much of the nanoceria to be filtered by kidneys as the average glomerular filtration pore diameter is about 75 nm, and the largest nanoceria dimension injected was no greater than 10 nm. However, urine collected during the first 24 hours after administration produced no detectable concentrations of nanoceria. It is possible that large nanoceria agglomorates form *in vivo* as seen in the TEM image of lysosomes found in the kidneys (Figure 3). Many nanoparticles in this image appear to be very small, but others appear to have agglomerated into much larger sizes of about 500 nm. While it is possible that these particles could cause kidney damage, it seems unlikely, as nanoceria concentrations in kidneys remained almost negligible and renal tissue did not show increased pathology compared to untreated controls. It is also possible that nanoceria was complexed to proteins such as albumin or that its negative charge prevented its filtration through the glomerular basement membrane (GBM). Additionally nanoceria may have been phagocytized and transported to the liver or spleen by macrophages to help reduce the filtered amount.

CONCLUSION

We have seen the ability of cerium oxide nanoparticles to scavenge ROS *in vitro*, their deposition and lack of pathology in mouse models, and their potential to reduce ROS *in vivo*. Given its regenerative nature and biodistribution, nanoceria may have the potential to be used as a treatment for oxidative stress.

4.4 MATERIALS AND METHODS

4.4.1. Synthesis of ceria nanoparticles

Cerium oxide nanoparticles were synthesized using simple wet chemistry methods. In a typical synthesis, a stoichiometric amount of cerium nitrate hexahydrate (99.999% from Sigma-Aldrich) was added to 50 mL of deionized water (18.2 M) and stirred for 1 h. The cerium(III) ions in the solution were oxidized to cerium(IV) oxide and the pH of the solution was kept below 3.5 to maintain the synthesized ceria nanoparticles in suspension. Crystalline nanoparticles of cerium oxide form immediately upon oxidation.

4.4.2. Cell culture and treatment

All cellular studies were conducted with a murine J774A.1 macrophage cell line (ATCC) incubated in culture using Dulbecco's modified Eagle medium (DMEM) 1 × media (Mediatech) supplemented with fetal bovine serum (FBS) (10%) (Hyclone) and penicillin/streptomycin (1%) (Mediatech). Cells were incubated at 37 °C with 5% CO2 and 95% air. For all experiments, cells were plated in 6-well plates at 2.5 × 105 cells mL-1. For nanoceria treatment or pretreatment, cells were incubated with the specified concentration of nanoceria in a fresh cell culture medium for 24 h. For cell stimulation, old medium was removed and replaced medium supplemented with lipopolysaccharide

(LPS) (1 μL mL-1) (Sigma) and reconstituted IFN- (Accurate Chemical) (100 U mL-1). Cells were incubated for another 24 h.

4.4.3. *In vitro* antioxidant measurements

Supernatants from cells undergoing nanoceria pretreatment and stimulation (described above) were collected. A Greiss assay was performed in which 50 ul of sample was transferred to a 96 well ELISA plate (Costar), 50 ul of 1% sulfanilamide (Sigma) dissolved in 100 mL 2.5% phosphoric acid (H_3PO_4) (Sigma) was added to each well, and 50 ul of 0.1% naphtylethylenediame (Sigma) dissolved in 100 mL 2.5% H_3PO_4 was added to each well. The same procedure was performed using standards of varying concentrations generated from $NaNO_2$ (Sigma). The plate was centrifuged to eliminate bubbles, all measurements were performed in triplicate, and averages of five separate tests were used to generate error statistics. Plates were read using an ELISA reader (Molecular Devices, Spectra Max 340PC) at 550 nm.

4.4.4. Experimental design: bio-distribution

Thirty-six, 8-week-old, CD-1 mice were divided into 2 major groups: 18 mice in group 1 received 2 injections spaced a week apart and 18 mice in group 2 received 5 injections also spaced a week apart. Each of the two groups contained 3 subgroups of 6 mice each that received one of 3 routes of administration (PO, IV, or IP). Each subgroup had 3 test mice and 3 control mice. In all, six subgroups were used as controls and were exposed to either 2 or 5 doses (2-week exposure or 5-week exposure respectively) of 100 μl sterile saline. The other six subgroups were used as the test groups exposed to either 2 or 5 doses (2-week exposure or 5-week exposure respectively) of 0.5 mg/kg of nanoceria suspended in 100 μl of sterile saline. Both major groups were given one injection a week

for either 2 or 5 weeks and were correspondingly necropsied on either weeks 3 or 6 of the study.

Immediately before euthanasia of mice, blood was collected and complete blood counts were performed for each mouse. Major organs (brain, heart, lung, liver, pancreas, spleen, stomach, small intestine and large intestine) were harvested and placed in 10% buffered formaldehyde. Tissue sections were then prepared for HRTEM, histopathology, or ICP-MS. A one way ANOVA test was used for analysis of the blood count.

4.4.5. Pathology and immune response

Tissue sections were placed in 10% buffered formaldehyde. Tissues were then trimmed, processed, stained with hematoxylin and eosin for histopathology, and scored on a scale from 0 to 4, based on severity of histopathologic changes (0=unremarkable, 1=minimal changes <5% of organ affected, 2= mild, 5–15% of organ affected, 3=moderate, 16–40% of organ affected, 4 =marked, >40% of organ affected). For WBC counts, blood was collected microtubes lined with an anticoagulant (product name and co) and a Unopette (co) was used to dilute blood, lyse RBC, and transfer an equal amount of solution to a hemacytometer plate to be counted manually as per the manufacturer's protocol. All counts were performed in quadruplicate and averaged for a final count.

4.4.6. Determining cellular uptake and biodistribution

HRTEM images of samples were obtained using a Zeiss 10 CA electron microscope. After nanoceria administration, tissues from mice were fixed as previously reported,[34] and tissue was then embedded in paraffin by an established protocol[35] and examined at an energy of 60 keV.

To determine biodistribution, organs were harvested and immediately placed in 10% buffered formaldehyde until ready to be examined. Tissues were later patted dry,

weighed and placed in 70% nitric acid overnight to start the digestion process. Samples were then microwave digested in an Xpress Microwave Digester. The temperature was ramped to 200 °C over 20 minutes and held there for another 20. Samples were then boiled down to less than 1 mL each and reconstituted in water to 10 mL exactly, and then Ce levels were assessed using inductively coupled plasma mass spectroscopy (ICP-MS).

Biodistribution was also assessed using an IVIS imaging station. Specially prepared FAM-tagged nanoceria was injected at either 2.5 or 5.0 mg/kg concentrations intravenously into CD1 mice. Images were taken at an f-stop of 4 with 2-second exposures at an excitation of 385 nm and emission of 509 nm. PBS injected controls were used to eliminate background noise and auto-fluorescence.

4.4.5. Experimental design: nanoceria as an *in vivo* antioxidant

Thirty BALB/c mice in groups of 10 were administered PBS, nanoceria (0.5 mg/kg), or NAC (1 g/kg) on weeks 1 and 2. Food was removed 12 hours before initial injections and returned to mice 8 hours post injection because food consumption may increase oxidative stress markers. On week 2, half of the mice in each group were given carbon tetrachloride (CCl_4) IP injections (200 mg/kg) 2 hours after their initial injections to induce liver toxicity. The other half was given PBS sham injections. Immediately after IP injections, all mice were placed in metabolic cages to collect urine, and three hours after IP injections, blood was collected from all mice. Urine samples were collected for each group for seven hours post CCl_4 injections. The same procedures were carried out with all mice on week 3 except that the only injections mice received were IP injections, and that the mice were euthanized after collection of urine. Livers were then collected from mice after euthanization, were snap frozen in liquid nitrogen, and all samples were placed in -80 °C for later analysis.

4.4.9. Measuring markers of oxidative stress

8-OH-dG levels indicative of DNA damage (particularly guanosine) was assessed in urine collected for 7 hours post CCl_4 injections. An 8-hydroxy-2-deoxy Guanosine EIA kit (Cayman Chemical) with included protocol and reagents was used and urine samples were normalized to creatinine levels using a colorimetric Creatinine Assay Kit (Cayman). Readings from all above assays were analyzed using a Molecular Devices Spectra Max 340PC reader. MDA levels were analyzed in mouse plasma using a TBARS Assay Kit (Cayman). The fluorimetric assay with higher sensitivity as opposed to the colorimetric assay was utilized and measured using a Molecular Devices Spectra Max Gemini XPS reader. 8-iso levels in whole livers were determined using an 8-Isoprostane EIA Kit (Cayman) and again measured using a Spectra Max 340PC reader. Homogenized liver samples were previously purified using SPE cartridges (Cayman) according to the 8-Iso EIA kit protocol.

ACKNOWLEDGEMENTS

Dr. Reilly acknowledges Beverly Rzigalinski, Ph.D. for her assistance in the initial phases of the project, her insightful comments, and her assistance in obtaining extramural funding for the project. This work was funded by the Arthritis Foundation and the National Institute of Health (1 R15 AI072756-01A2).

4.5 LITERATURE CITED

[1] N. Fujiwara, K. Kobayashi, *Curr Drug Targets Inflamm Allergy* **2005**, *4*, 281.
[2] I. Juranek, S. Bezek, *Gen Physiol Biophys* **2005**, *24*, 263.

[3] B. A. Rzigalinski, K. Meehan, R. M. Davis, Y. Xu, W. C. Miles, C. A. Cohen, *Nanomed* **2006**, *1*, 399.
[4] I. P. Kaur, T. Geetha, *Mini Rev Med Chem* **2006**, *6*, 305.
[5] O. I. Shadyro, I. L. Yurkova, M. A. Kisel, *Int J Radiat Biol* **2002**, *78*, 211.
[6] R. W. Tarnuzzer, J. Colon, S. Patil, S. Seal, *Nano Lett* **2005**, *5*, 2573.
[7] H. Sies, *Exp Physiol* **1997**, *82*, 291.
[8] M. R. McCall, B. Frei, *Free Radic Biol Med* **1999**, *26*, 1034.
[9] B. Halliwell, *Annu Rev Nutr* **1996**, *16*, 33.
[10] C. Kerksick, D. Willoughby, *J Int Soc Sports Nutr* **2005**, *2*, 38.
[11] G. B. Corcoran, B. K. Wong, *J Pharmacol Exp Ther* **1986**, *238*, 54.
[12] C. H. Jackson, N. C. MacDonald, J. W. Cornett, *Can Med Assoc J* **1984**, *131*, 25.
[13] G. Wu, Y. Z. Fang, S. Yang, J. R. Lupton, N. D. Turner, *J Nutr* **2004**, *134*, 489.
[14] P. Takacs, S. W. Kauma, M. M. Sholley, S. W. Walsh, M. J. Dinsmoor, K. Green, *FASEB J* **2001**, *15*, 279.
[15] M. F. Hochella, Jr., S. K. Lower, P. A. Maurice, R. L. Penn, N. Sahai, D. L. Sparks, B. S. Twining, *Science* **2008**, *319*, 1631.
[16] M. Nolan, S. C. Parker, G. W. Watson, *Phys Chem Chem Phys* **2006**, *8*, 216.
[17] M. Nolan, S. C. Parker, G. W. Watson, *J Phys Chem B Condens Matter Mater Surf Interfaces Biophys* **2006**, *110*, 2256.
[18] B. A. Rzigalinski, *Technol Cancer Res Treat* **2005**, *4*, 651.
[19] C. Korsvik, S. Patil, S. Seal, W. T. Self, *Chem Commun (Camb)* **2007**, 1056.
[20] M. Das, S. Patil, N. Bhargava, J. F. Kang, L. M. Riedel, S. Seal, J. J. Hickman, *Biomaterials* **2007**, *28*, 1918.
[21] J. Chen, S. Patil, S. Seal, J. F. McGinnis, *Nat Nanotechnol* **2006**, *1*, 142.
[22] J. Chen, S. Patil, S. Seal, J. F. McGinnis, *Adv Exp Med Biol* **2008**, *613*, 53.
[23] S. M. Hirst, A. S. Karakoti, R. D. Tyler, N. Sriranganathan, S. Seal, C. M. Reilly, *Small* **2009**, *5*, 2848.
[24] M. B. Kadiiska, B. C. Gladen, D. D. Baird, D. Germolec, L. B. Graham, C. E. Parker, A. Nyska, J. T. Wachsman, B. N. Ames, S. Basu, N. Brot, G. A. Fitzgerald, R. A. Floyd, M. George, J. W. Heinecke, G. E. Hatch, K. Hensley, J. A. Lawson, L. J. Marnett, J. D. Morrow, D. M. Murray, J. Plastaras, L. J. Roberts, 2nd, J. Rokach, M. K. Shigenaga, R. S. Sohal, J. Sun, R. R. Tice, D. H. Van Thiel, D. Wellner, P. B. Walter, K. B. Tomer, R. P. Mason, J. C. Barrett, *Free Radic Biol Med* **2005**, *38*, 698.
[25] M. A. Balboa, J. Balsinde, *Biochim Biophys Acta* **2006**, *1761*, 385.
[26] T. X. Sayle, S. C. Parker, D. C. Sayle, *Phys Chem Chem Phys* **2005**, *7*, 2936.
[27] E. G. Heckert, A. S. Karakoti, S. Seal, W. T. Self, *Biomaterials* **2008**, *29*, 2705.
[28] F. H. Scholes, C. Soste, A. E. Hughes, S. G. Hardin, P. R. Curtis, *Applied Surface Science* **2006**, *253*, 1770.
[29] F. H. Scholes, A. E. Hughes, S. G. Hardin, P. Lynch, P. R. Miller, *American Chemical Society* **2007**, *19*, 2321.
[30] J. Guzman, S. Carrettin, A. Corma, *J Am Chem Soc* **2005**, *127*, 3286.
[31] M. B. Kadiiska, B. C. Gladen, D. D. Baird, L. B. Graham, C. E. Parker, B. N. Ames, S. Basu, G. A. Fitzgerald, J. A. Lawson, L. J. Marnett, J. D. Morrow, D. M. Murray, J. Plastaras, L. J. Roberts, 2nd, J. Rokach, M. K. Shigenaga, J. Sun, P. B. Walter, K. B. Tomer, J. C. Barrett, R. P. Mason, *Free Radic Biol Med* **2005**, *38*, 711.
[32] K. S. Lee, M. Buck, K. Houglum, M. Chojkier, *J Clin Invest* **1995**, *96*, 2461.
[33] A. Virdis, M. F. Neves, F. Amiri, E. Viel, R. M. Touyz, E. L. Schiffrin, *Hypertension* **2002**, *40*, 504.

[34] *Poly/Bed 812 Data Sheet*, PolySciences, Inc.
[35] M. J. Dykstra, L. E. Reuss, *Microscopy: Theory, Techniques, and Troubleshooting* **2003**, *2*, 109.

Chapter 5

5.1 SUMMARY AND CONCLUSIONS

For the past couple of decades, oxidative stress has been implicated as a contributing factor in numerous diseases.[1] Overabundant free radicals and reactive oxygen species (ROS) that cause oxidative stress are a major concern due to their nature to damage cellular constituents and cause widespread tissue damage.[1] ROS react indiscriminately, stripping electrons from nearby molecules whether they are proteins, carbohydrates, lipids, or DNA. Damage can result in cell death or the disruption of cellular functions and homeostasis.[2, 3] Acute oxidative stress is a useful mechanism to combat microbial disease, however in chronic oxidative stress the body loses its ability to repair tissue damage.[1] While it is unknown whether oxidative stress contributes to or is a symptom of disease, its treatment is necessary to help prevent tissue damage and cellular death.

Oxidative stress treatments are typically non-enzymatic antioxidants. Antioxidants are naturally found in our foods and produced in our bodies, however under conditions of oxidative stress they are not consumed or produced in sufficient quantities to combat ROS.[4] Antioxidant treatments are often given orally and must be continually replenished to maintain efficacy. Vitamins C and E and N-acetyl cysteine are examples of commonly administered antioxidants.[5] They function by intercepting ROS and cellular targets, offering or accepting electrons and quenching ROS to non-reactive or less reactive products.[6] Some antioxidants are water soluble and therefore quickly excreted, and some have short half-lives and lose their abilities to quench ROS within hours of

consumption.[5] While these antioxidant treatments are helpful, they cannot be maintained at sufficient concentrations to combat oxidative stress efficiently.

We have investigated cerium oxide nanoparticles as a potential treatment for oxidative stress due to their inherent abilities to quench ROS and auto-regenerate their antioxidant characteristics. Cerium oxide has many oxygen defects in is lattice structure when manufactured on the nanoscale. Due to its oxygen defects, nanoceria is able to donate and accept electrons, acting as an antioxidant, switching back and forth between its 3+ and 4+ oxidation states.[7, 8] It has the capacity to auto-regenerate and the ability to return to a more favorable 3+ oxidation state after being oxidized by ROS.

Our goal in these studies was to investigate the antioxidant properties of nanoceria *in vitro* and *in vivo,* and to determine the biodistribution and biocompatibility of nanoceria treatments in murine models. *In vitro,* we found that nanoceria was capable of scavenging ROS, namely nitric oxide (NO), and reducing iNOS mRNA and protein. Our *in vivo* results showed favorable nanoceria deposition in the spleens and livers of nanoceria administered mice, without pathologic findings, although WBC levels increased. We also measured markers of oxidative stress in mice treated with nanoceria and with induced ROS production. Our results are promising but not yet conclusive as to whether nanoceria can reduce ROS *in vivo*. Due to the antioxidant behavior of nanoceria *in vitro* and its biocompatibility *in vivo,* we feel that nanoceria has the potential to be investigated further as a treatment for oxidative stress.

5.2. LITERATURE CITED

[1] I. Juranek, S. Bezek, *Gen Physiol Biophys* **2005**, *24*, 263.
[2] I. P. Kaur, T. Geetha, *Mini Rev Med Chem* **2006**, *6*, 305.
[3] O. I. Shadyro, I. L. Yurkova, M. A. Kisel, *Int J Radiat Biol* **2002**, *78*, 211.
[4] C. Kerksick, D. Willoughby, *J Int Soc Sports Nutr* **2005**, *2*, 38.
[5] B. Halliwell, *Annu Rev Nutr* **1996**, *16*, 33.
[6] H. Sies, *Exp Physiol* **1997**, *82*, 291.
[7] B. A. Rzigalinski, K. Meehan, R. M. Davis, Y. Xu, W. C. Miles, C. A. Cohen, *Nanomed* **2006**, *1*, 399.
[8] S. M. Hirst, A. S. Karakoti, R. D. Tyler, N. Sriranganathan, S. Seal, C. M. Reilly, *Small* **2009**, *5*, 2848.

APPENDIX 1

LIST OF CITATIONS

Figure 2.1 [fair use]
Inflammation. Last modified 16 November 2007. http://users.rcn.com/jkimball.ma.ultranet/BiologyPages/I/Inflammation.html (accessed Feb. 10, 2010)

Figure 2.2 [fair use]
Reactive Oxygen Species (ROS). Last modified 9 July 2008. http://users.rcn.com/jkimball.ma.ultranet/BiologyPages/R/ROS.html (accessed Feb. 10, 2010)

Figure 2.3 [used with permission]

8-Istoprostane EIA Kit booklet: Formation of 8-Isoprostane image on page 6. Copyright 26 October 2009, Cayman Chemical Company, Ann Arbor, MI.

Figure 2.4 [used with permission]
McCall and Frei. Free Radical Biology & Medicine, Vol. 26, Nos. 7/8, pp. 1034 –1053, 1999. Fig. 1. Chemical structure of the "antioxidant vitamins" (B-carotene, vitamins E and C). Copyright © 1999 Elsevier Science Inc.

Figure 2.5 [fair use]
Ben Best. N-AcetylCysteine (NAC). http://www.benbest.com/nutrceut/NAC.html. All writing on this website is copyrighted (c) by Ben Best year 1990 or later. Permission freely given to quote or copy written material provided the source URL is provided.

Figure 2.6 (left) [fair use]
The Immune System: Physical Barriers. http://www.odec.ca/projects/2007/sank7b2/page7.html (Accessed on Feb. 10, 2010).

Figure 2.6 (right) [used with permission]
Adapted by permission from Macmillan Publishers Ltd: [Nature Reviews Molecular Cell Biology] 4, 385-396 (Copyright May 2003). Rosenberger and Finlay. Phagocyte sabotage: disruption of macrophage signaling by bacterial pathogens. http://www.nature.com/nrm/journal/v4/n5/fig_tab/nrm1104_F2.html (Accessed on Feb. 10, 2010).

Figure 2.7 [used with permission]
McCall and Frei. Free Radical Biology & Medicine, Vol. 26, Nos. 7/8, pp. 1034 –1053, 1999. Fig. 2. Chemical structure of selected lipid peroxidation products (A–C) and selected oxidized purine bases (D, E). Copyright © 1999 Elsevier Science Inc.

Chapter 3 [used with permission]
Suzanne M Hirst, Ajay S. Karakoti, Ron D. Tyler, Nammalwar Sriranganathan, Sudipta Seal, and Christopher M. Reilly: Anti-inflammatory effects of cerium oxide

nanoparticles. Small. 2009. Volume 5, Pages 2848-2857. Copyright Wiley-VCH Verlag GmbH & Co. KGaA. Reproduced with permission.

All remaining figures, graphs, images and tables were created by the author Suzanne Hirst.